MEHP/ethanol co-exposure favors the death of steatotic hepatocytes, possibly through CYP4A and ADH involvement

Arnaud Tête, Isabelle Gallais, Muhammad Imran, Louis Legoff, Corinne Martin-Chouly, Lydie Sparfel, Maelle Bescher, Odile Sergent, Normand Podechard, Dominique Lagadic-Gossmann

CREDIT AUTHORSHIP CONTRIBUTION STATEMENT

Arnaud Tête: Investigation, Formal analysis, Visualization, Writing - original draft ; **Isabelle Gallais**, **Muhammad Imran** : Investigation, Formal analysis, Visualization, Writing - review & editing; **Corinne Martin-Chouly, Lydie Sparfel**: Methodology, Writing - review & editing ; **Louis Legoff, Maëlle Bescher**: Investigation; **Odile Sergent** : Conceptualization, Methodology, Writing - review & editing, Supervision ; **Normand Podechard** : Conceptualization, Methodology, Formal analysis, Funding acquisition, Supervision; **Dominique Lagadic-Gossmann**: Conceptualization, Formal analysis, Visualization, Writing - original draft, Writing - review & editing, Funding acquisition, Supervision, Project administration.

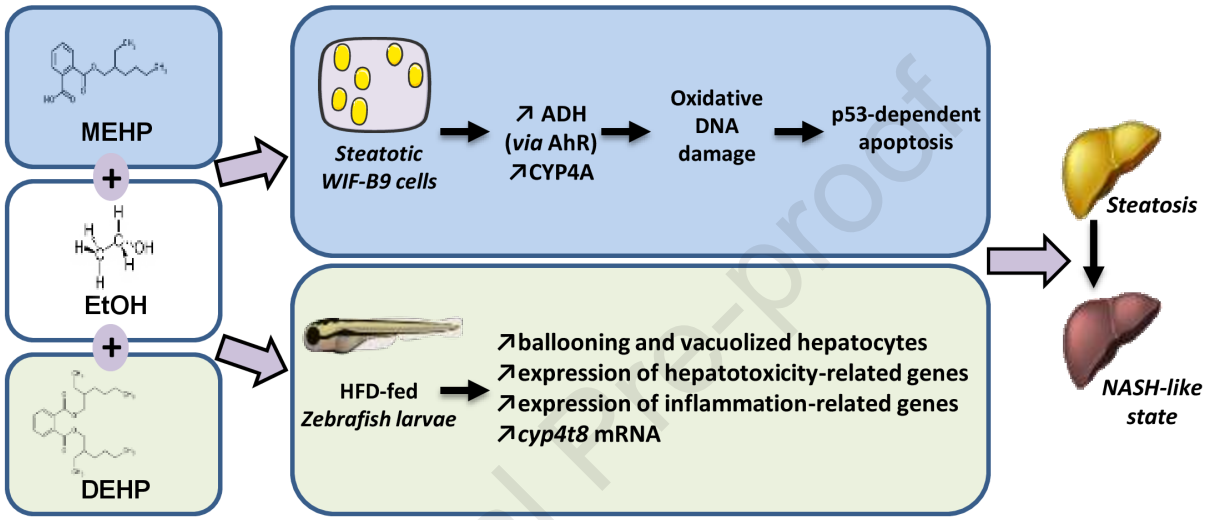

MEHP/ethanol co-exposure favors the death of steatotic hepatocytes, possibly through CYP4A and ADH involvement

Arnaud Tête[1,*], Isabelle Gallais[*], Muhammad Imran, Louis Legoff, Corinne Martin-Chouly, Lydie Sparfel, Maëlle Bescher, Odile Sergent[#], Normand Podechard[#], Dominique Lagadic-Gossmann[#$]

Univ Rennes, Inserm, EHESP, Irset (Institut de recherche en santé, environnement et travail) - UMR_S 1085, F-35000 Rennes, France

[1]Present address : INSERM UMR-S 1124, Université de Paris, 45 rue des Saints-Pères, 75006 Paris, France

* : equal contribution

: equal supervision

$: **Corresponding author** at IRSET / Inserm U1085, Université Rennes 1, Faculté de Pharmacie, 2 avenue du Professeur Léon Bernard, 35043 Rennes cedex, France. E-mail : dominique.lagadic@univ-rennes1.fr – Tel : +33(0)223234837

Key words: NAFLD; DEHP; AhR; DNA damage; oxidative stress; Zebrafish larvae

Abbreviations: ADH: alcohol dehydrogenase; AhR: Aryl Hydrocarbon Receptor; CYP: cytochrome P450; DEHP: di(2-ethylhexyl) phthalate; dpf: days post-fertilization; EtOH: ethanol; HFD: high fat diet; MDA: Malondialdehyde; MEHP: Mono(2-ethylhexyl) phthalate; NAFLD; nonalcoholic fatty liver disease; NASH: nonalcoholic steatohepatitis

HIGHLIGHTS

1-MEHP/EtOH co-exposure leads to death of steatotic hepatocytes *via* oxidative DNA damage.

2-MEHP-activated AhR would enhance ethanol metabolism by ADH in steatotic cells.

3-The toxicity by MEHP/EtOH co-exposure would rely on CYP4A activity in steatotic cells.

4-Co-exposure to DEHP/EtOH of HFD-zebrafish larva induces progression of liver steatosis.

ABSTRACT

Liver steatosis has been associated with various etiological factors (obesity, alcohol, environmental contaminants). How those factors work together to induce steatosis progression is still scarcely evaluated. Here, we tested whether phthalates could potentiate death of steatotic hepatocytes when combined with ethanol. Pre-steatotic WIF-B9 hepatocytes were co-exposed to mono(2-ethylhexyl) (MEHP, 500 nM; main metabolite of di(2-ethylhexyl) phthalate or DEHP) and ethanol (5 mM) for 5 days. An increased apoptotic death was detected, involving a DNA damage response. Using 4-Methypyrazole to inhibit ethanol metabolism, and CH-223191 to antagonize the AhR receptor, we found that an AhR-dependent increase in alcohol dehydrogenase (ADH) activity was essential for cell death upon MEHP/ethanol co-exposure. Toxicity was also prevented by HET0016 to inhibit the cytochrome P450 4A (CYP4A). Using the antioxidant thiourea, a role for oxidative stress was uncovered, notably triggering DNA damage. Finally, co-exposing the *in vivo* steatosis model of high fat-diet (HFD)-zebrafish larvae to DEHP (2.56 nM)/ethanol (43 mM), induced the pathological progression of liver steatosis alongside an increased *Cyp4t8* (human CYP4A homolog) mRNA expression. Altogether, these results further emphasized the deleterious impact of co-exposures to ethanol/ environmental pollutant towards steatosis pathological progression, and unraveled a key role for ADH and CYP4A in such effects.

1-INTRODUCTION

Non-Alcoholic Fatty Liver Disease (NAFLD) is the most common form of chronic liver disease worldwide, with about 25% of the global population affected, reaching up to 80% in over-weight or obese people (Younossi *et al*., 2016b; Chalasani *et al*., 2018). Moreover, its occurrence is steadily rising, along with obesity epidemics that represents the main risk factor for these diseases (Younossi *et al*., 2016b; Estes *et al*., 2018). NAFLD encompasses a large spectrum of hepatic lesions from fatty liver (steatosis) to Non-Alcoholic Steatohepatitis (NASH) that can exhibit different degrees of severity depending on fibrotic status (Chalasani *et al*., 2018; Patel *et al*., 2016). Steatosis is characterized by lipid accumulation in the liver, evidenced by the formation of triglyceride-containing lipid droplets in hepatocytes (Sahini and Borlak, 2014; Sanyal *et al*., 2011), while in NASH, this state is accompanied with death of hepatocytes and inflammation (Sanyal *et al*., 2011). NASH is known to form a favorable ground to cirrhosis and hepatocellular carcinoma (HCC) development (Ekstedt *et al*., 2006; Younossi *et al*., 2015). Consequently, NAFLD has become a leading cause of HCC development and has been associated with an increased risk of mortality (Younossi *et al*., 2015, 2016a). In this context, whereas steatosis is not harmful by itself, it can be considered as a liver sensitizing stage to external aggressions inducing cell death and/or inflammation, thereby favoring pathological progression to NASH and more. Of note, about 10 to 20% of people with steatosis have been reported to develop NASH thereafter (Estes *et al*., 2018; Siegel *et al*., 2009). However, the nature of these aggressions and the related molecular mechanisms are yet not fully known.

Hepatic steatosis has been associated with various etiological factors including obesity, alcohol and environmental contaminants (Foulds *et al*., 2017). Regarding these latter factors, several studies have indeed highlighted a potential implication of environmental chemicals in NAFLD development and progression, by altering lipid metabolism or inducing cell injuries in liver (Foulds *et al.*, 2017; Heindel *et al*., 2017). This is in this context that NAFLD caused by environmental toxicants has been called TAFLD, for Toxicant-Associated Fatty Liver Disease, and TASH, for Toxicant-Associated Steatohepatitis (Wahlang *et al*., 2013, 2019). However, the impact on liver of combinations of various etiological factors is still scarcely evaluated despite the fact that it further mimics the real

life. Thus, we have previously demonstrated that co-exposure to alcohol, a well-known lifestyle hepatotoxicant, and the environmental carcinogen benzo[*a*]pyrene (B[*a*]P), can drive the progression of a pre-established steatosis to a NASH-like state both *in vitro* and *in vivo* (Bucher *et al*., 2018a, 2018b; Imran *et al*., 2018; Tête *et al*., 2018). In these studies, we have notably demonstrated that B[*a*]P/ethanol co-exposure induced apoptotic death of steatotic hepatocytes through several mechanisms including changes in xenobiotic metabolism, oxidative stress notably leading to oxidative DNA damage and lipid peroxidation, and an AhR (Aryl Hydrocarbon Receptor)-dependent mitochondrial dysfunction (Bucher *et al*., 2018a; Tête *et al*., 2018). In addition, we found that membrane remodeling was involved in liver steatosis progression in High Fat Diet (HFD)-fed zebrafish larvae (Imran *et al*., 2018).

Many other toxicants have been demonstrated or are suspected to be metabolism-disrupting chemicals, and therefore could also be involved in the development of NAFLD (Al-Eryani *et al*., 2015; Heindel *et al*., 2017; Le Magueresse-Battistoni *et al*., 2017). Among these pollutants, phthalates and especially Di(2-Ethylhexyl) Phthalate (DEHP) are frequently cited (Benjamin *et al*., 2017; Foulds *et al*., 2017; Heindel *et al*., 2017). DEHP is commonly used as a plasticizer of Polyvinyl Chloride (PVC) industry and is ubiquitous in environment (Benjamin *et al*., 2017). Human exposure to phthalates is mainly through diet because they can readily be leached from plastic packaging to foods and drinks since not chemically-bound to polymers (Benjamin *et al*., 2017; Wang *et al*., 2019). In the organism, DEHP is rapidly metabolized in the gut to Mono(2-Ethylhexyl) Phthalate (MEHP); this metabolite that is considered as the active metabolite for metabolic disruption upon DEHP exposure, then goes to the liver (Frederiksen *et al*., 2007; Keys *et al*., 1999). Thus, DEHP and/or MEHP have been reported as disturbing lipid metabolism both *in vitro* in human hepatic cells (Bai *et al*., 2019; Zhang *et al*., 2017b, 2019) and *in vivo* in adult male zebrafish (Huff *et al*., 2018). In these *in vitro* studies, MEHP was able to induce an oxidative stress, thereby affecting cell viability at high exposure concentrations $\geq$ 50 µM (Bai *et al*., 2019; Zhang *et al*., 2019). Regarding the *in vivo* experiment in zebrafish, a low concentration of DEHP (5.8 nM) was tested, revealing modulations of expression of liver genes related to fatty acid metabolism and development of NAFLD (Huff *et al*., 2018). DEHP was also demonstrated to exacerbate NAFLD *in vivo*, in rats fed with HFD (Chen *et al*., 2016), while

MEHP exposure was described as possibly related to NAFLD development in human (Milošević *et al*., 2020). Regarding co-exposure of DEHP with ethanol, only the interaction of this phthalate with ethanol metabolism in liver was reported (Agarwal *et al*., 1982), and a very recent study pointed to a synergistic effect of both molecules towards unsaturated fatty acid synthesis in liver (Li *et al*., 2020). However, nothing has so far been reported regarding the pathological progression of prior liver steatosis upon such a co-exposure.

In the present study, we have therefore decided to analyze the impact of phthalate/ethanol co-exposure on such a progression. To this aim, we have tested the effects of MEHP/ethanol co-exposure *in vitro* on pre-steatotic WIF-B9 hepatocytes, and of DEHP/ethanol co-exposure *in vivo* in HFD-fed zebrafish larvae. Our present *in vitro* data show that MEHP/ethanol co-exposure at low doses results in the apoptotic death of steatotic hepatocytes, notably through oxidative DNA damage and p53 activation. Cooperative mechanistic interactions between ethanol and MEHP metabolisms have been highlighted, involving not only an AhR-dependent activation of Alcohol Dehydrogenase (ADH) but also cytochrome P450 4A (CYP4A). Besides hepatocyte damage, DEHP/ethanol co-exposure of HFD-zebrafish larvae leads to signs of inflammation. In conclusion, exposure to DEHP or MEHP in combination with ethanol could favor the pathological progression of NAFLD.

2-MATERIAL AND METHODS

2.1- Chemicals and antibodies

Chlorzoxazone (CZX), 1-Methyl-N-[2-methyl-4-[2-(2-methylphenyl) diazenyl]phenyl-1H-pyrazole-5-carboxamide (CH-223191), Di(2-ethylhexyl) phthalate (DEHP), N-acetyl-Asp-Glu-Val-Asp-7-amido-4-methylcoumarin (Ac-DEVD-AMC), 7-ethoxyresorufin, HET0016 (SLL2416), Hoechst-33342, Mono(2-ethylhexyl) phthalate (MEHP), 4-methylpyrazole (4-MP), (3-(4,5-dimethylthiazol-2-yl)-2,5-diphenyltetrazolium bromide) (MTT), β-nicotinamide adenine dinucleotide (NADH), α-Naphthoflavone (αNF), pifithrine-α (PFT), salicylamide and thiourea were all obtained from Sigma-Aldrich (Saint Quentin Fallavier, France). Ethanol (EtOH; purity: 99.97%) used for treatment was purchased from Prolabo (Paris, France). N-benzyloxycarbonyl-Val-Ala-Asp-(O-Me) fluoromethyl ketone (zVAD-FMK) was acquired from Calbiochem (Millipore, Saint-Quentin Les Yvelines, France). Sytox® green was obtained from Invitrogen, (Cergy Pontoise, France). [^{3}H]-thymidine was purchased from Amersham Biosciences (Buck, United Kingdom). 6-Hydroxy Chlorzoxazone (6-OH-CZX) and Chlorzoxazone O-Glucuronide (OCZX) were acquired from Toronto Research Chemicals (North York, Canada). Chlorzoxazone N-Glucuronide (NCZX) was obtained from Bertin Pharma (Montigny-le-Bretonneux, France).

Antibodies used for immunofluorescence and western blotting experiments were as follows: mouse monoclonal anti-CYP4A (A1/A2/A3) (sc-53247) and mouse monoclonal anti-HSC70 (sc-7298) both purchased from Santa Cruz Biotechnology (Heidelberg, Germany) ; mouse monoclonal anti-phospho-H2AX (Ser139) (05-636) antibody was acquired from Merck Millipore (Molsheim, France); mouse monoclonal anti-p53 (#2524S) and anti-phospho-p53 (Ser15; #12571), as well as caspase-3 (3G2) mouse antibody (#9668) were obtained from Cell Signaling Technology (Saint Quentin, France). Alexa Fluor FITC-conjugated secondary antibodies were purchased from Invitrogen (Cergy Pontoise, France) and secondary antibodies conjugated with horseradish peroxidase were from DAKO (Les Ulis, France).

2.2- WIF-B9 cell culture and treatments

WIF-B9 hepatic hybrid cell line, obtained by fusion of Fao rat hepatoma cells and WI-38 human fibroblasts (Decaens *et al*., 1996) was a generous gift from Dr Doris Cassio (UMR Inserm S757, Université Paris-Sud, Orsay, France). WIF-B9 cells were grown in F-12 Ham medium with Coon's modification supplemented with 5% fetal calf serum (Eurobio, Courtaboeuf, France), 2 mM glutamine, 100 U/mL penicillin, 0.1 mg/mL streptomycin, 0.25 µg/mL amphotericin B, 0.22 g/L $NaHCO_3$, HAT (10 µM hypoxanthine, 40 nM aminopterin, 1.6 µM thymidine) and incubated at 37 °C in an atmosphere constituted of 5% CO_2. Before any treatment, cells were seeded at $12.5x10^3$ cells/cm^2 and cultured for 7 days until reaching approximately 80% of confluence.

Exposure protocol is given in supplementary Fig. S1A. Briefly, prior to chronic treatments with toxicants, steatosis was induced by a 2-days treatment with medium containing a fatty acids (450 µM oleic acid/100 µM palmitic acid)-albumin complex, as previously described (Bucher *et al*., 2018b). Cells with or without prior fatty acid supplementation were then exposed to sub-toxic concentrations of toxicants (500 nM MEHP and/or 5 mM ethanol). In case of co-treatment with inhibitors, they were added to culture medium for 1h prior to co-treatments with toxicants.

2.3- Zebrafish Larvae Handling and treatments

Animals were handled, treated and killed in agreement with the European Union regulations concerning the use and protection of experimental animals (Directive 2010/63/EU). All protocols were approved by local ethic committee CREEA (Comité Rennais d'Éthique en matière d'Expérimentation Animale, Rennes, France; approval number R-2012-NP-01). Fertilized zebrafish embryos collected following natural spawning were obtained from the Structure Fédérative de Recherche Biosit (Inrae LPGP, Rennes, France). Embryos and larvae (sex unknown) were raised at 28 °C according to standard procedures and as previously described (Podechard *et al*., 2017). Exposure protocol is given in supplementary Fig. S1B. Briefly, from 4 days post-fertilization (dpf) until 9 dpf, larvae were fed daily during 1 hour before medium renewal with a Standard Diet (SD) (10% of fat) (Tetramin, Tetra, Blacksburg, VA, USA), or with a High Fat Diet (HFD) (~53% of fat) (Sigma-Aldrich, St. Louis, MO, USA). Validation of the protocol to induce liver steatosis has been previously published (Bucher *et a*l., 2018; Imran *et al*., 2018); of note, a clear lipid accumulation was detected as soon as 1 day of HFD.

Based upon our exposure protocol (see supplementary Fig. S1B), one might thus expect all larvae to exhibit liver steatosis at the time of killing. Concerning toxicant exposure, at 5 dpf, larvae were treated with 2.56 nM DEHP and/or 43 mM ethanol directly added to the incubation medium. Regarding the choice of ethanol concentration, it was based on previous work estimating an internal dose of 10 mM following larvae exposure to 43 mM ethanol (data not shown). With respect to DEHP, the choice of concentration was based first on human exposure (2.54 and 2.85 µg/kg body weight per day for adult female and male, respectively; Wormuth *et al*., 2006), second on previous work on zebrafish showing modulation of fatty acid metabolism in liver with 2.26 µg/L (5.8 nM) DEHP (Huff *et al*., 2018). As *in vivo* treatments were longer than *in vitro*, a lower concentration of DEHP compared to the *in vitro* MEHP concentration was thus tested on zebrafish larvae.

2.4- WIF-B9 viability, cell death and proliferation evaluation

In order to select MEHP concentration used for the experiments, a cell viability dose-response was assessed by MTT test with non steatotic WIF-B9. After exposure to different concentrations of MEHP, cells were incubated at 37 °C for 1 hour with a 0.5 mg/mL MTT solution (in a serum-free and DMSO-free medium). After washing, cells were then lysed with DMSO and absorbance at 540 nm was measured (POLARstar Omega microplate reader; BMG Labtech, ThermoFisher Scientific, France).

Apoptotic and necrotic cell death was assessed by fluorescence microscopic observation after Hoechst/Sytox green staining, as previously described (see Tête *et al*., 2018, for details).

Measurement of caspase-3/7 activity assays were performed using Ac-DEVD-AMC tetrapeptide fluorogenic substrate, as previously described (Collin *et al*., 2014). Briefly, after toxicant exposure, cells were lysed and 80 µg of protein were then incubated with 80 µM DEVD-AMC at 37 °C for 2 hours. Measurement of caspase-mediated cleavage of DEVD-AMC was assessed by spectrofluorimetry (Spectramax Gemini; Molecular Devices, San Jose, California, United States).

Cell proliferation was assessed by [^{3}H]-thymidine cell incorporation. During the last 48h of toxicant exposure, cells were cultured in a medium containing 1 µCi [^{3}H]-thymidine/ml. Following

treatments, cells were scraped, and aliquoted for protein content determination and for [^{3}H]-thymidine incorporation measurement after precipitation in 30% trichloroacetic acid overnight at 4°C.

2.5- Histological analysis of liver toxicity in zebrafish larvae

Histological analysis was performed as previously described (Podechard *et al*., 2017). Briefly, after toxicant exposure, larvae were washed in PBS and fixed in 4% paraformaldehyde in PBS at 4 °C before being embedded in paraffin. Then, 5 µm sections were stained with Hematoxylin, Eosin and Safran red (HES) and imaged on a Nanozoomer NDP (Hamamatsu Photonics K.K., Hamamatsu, Japan) (magnification ×400). Histological analysis of dead or damaged cells (visualized as cellular dropouts, ballooning cells, and vacuolated hepatocytes) was assessed from images (2 or 3 sections) of at least 3 larvae per condition.

2.6- DNA damage and nuclear p53 expression evaluation by immunofluorescence

Immunofluorescence was used to analyze DNA damage and nuclear p53 expression. DNA damage was assessed by analyzing the H2AX phosphorylation on Ser139 (γ-H2AX), as previously described (Tête *et al*., 2017). Cells were counted as positive for DNA damage when they exhibit more than 5 nuclear γ-H2AX foci (>100 cells were analyzed per condition). Briefly, after incubation of fixed cells with 1:1000 diluted anti-γ-H2AX or 1:500 diluted anti-p53 antibody for 2 h at room temperature, they were next incubated with Alexa Fluor FITC-conjugated secondary antibodies for 2 h. After washing with PBS, nuclei were counterstained with 300 nM DAPI for 5 min. Finally, cells were analyzed using an automated microscope Leica DMRXA2 (Leica Microsystems, Wetzlar, Germany) with a 63× fluorescence objective.

2.7- Analysis of gene mRNA expression by RT-qPCR

mRNA gene expression analysis was performed as previously described (see Bucher *et al*., 2018b; Imran *et al*., 2018, for further details). mRNA expression was normalized by rat *β-actin* mRNA expression for WIF-B9 cells, and by means of actb2 and gapdh mRNA levels as well as of 18s rRNA levels for zebrafish larvae. The $2^{-\Delta\Delta Ct}$ method was used to express the relative expression of

each gene. Sequences of rat and zebrafish primers presently tested are provided in supplementary Tables S1 and S2, respectively.

2.8- Analysis of CYP4A protein expression by western blotting

After toxicant exposure, cells were harvested and sonicated on ice in RIPA buffer supplemented with a cocktail of protein inhibitors (Roche). After protein concentration determination, 30 μg of whole-cell lysates were then separated by sodium dodecyl sulfate–polymerase gel electrophoresis (SDS–PAGE). Gels were next electroblotted onto Amersham™ Protran® Western blotting membranes, overnight at 4°C. Membranes were next blocked with a Tris-buffered tween solution supplemented with 5% bovine serum albumin for 2 h and next hybridized with anti-CYP4A antibody overnight at 4 °C. They were then incubated with appropriate horseradish peroxidase-conjugated secondary antibodies for 1h, and immunolabeled proteins were visualized by chemiluminescence using the LAS-3000 analyzer (Fujifilm). For protein loading evaluation, a primary antibody anti-HSC70 was used. Images processing were performed using Multi Gauge software (Fujifilm). Note that similar protocols were applied for analyzing caspase-3 cleavage and p53 phosphorylation on Ser-15, with their respective antibodies.

2.9- Measurement of cytochrome P450s and ADH activities

CYP1, CYP2E1 and ADH activities were all assessed as previously described (Tête *et al*., 2018). Briefly, CYP1 activities were evaluated using the Ethoxyresorufin O-deethylase (EROD) assay, based on the conversion of ethoxyresorufin into resorufin by CYP1 enzymes. Regarding CYP2E1 activity, it was determined by analysis of the formation of chlorzoxazone O-glucuronide (OCZX) by a high-performance liquid chromatography (HPLC) method (see Tête *et al*., 2018, for details). To assess alcohol dehydrogenase (ADH) activity, measurement of the reduced form of β-nicotinamide adenine dinucleotide (β-NADH) stemming from ethanol oxidation in presence of the oxidized form β-NAD^+ was realized (see Tête *et al*., 2018, for details).

2.10- Detection of oxidative stress

2.10.1- Determination of ROS production. Intracellular ROS production was assessed using dihydroethidium (DHE), a fluorescent probe sensitive to superoxide anion. The fluorescence of 2-OH-ethidium (2-OH-E+) was analyzed, as previously described (Tête *et al*., 2018). Results were given as fluorescence arbitrary units (F.A.U.)/mg protein.

2.10.2- Evaluation of lipid peroxidation. Lipid peroxidation was assessed in culture media by measuring free malondialdehyde (MDA), a secondary end-product of lipid hydroperoxide decomposition. To this aim, an HPLC protocol was applied, as previously described (Tête *et al*., 2018).

2.11- Analysis of oxygen consumption and extracellular acidification rates

WIF-B9 cells were seeded in Seahorse XF 24-well microplates (Seahorse Bioscience, Agilent Technologies) at $12.5x10^3$ cells/cm^2. On the day prior to the experiment, XF extracellular flux cartridge was hydrated with XF calibrant overnight. After the 5 days-treatment, the medium was changed to assay medium (unbuffered DMEM with 10 mM glucose, 2 mM glutamine, 2 mM pyruvate), and kept 1h in a non-CO_2 incubator at 37 °C. The mitochondrial function assay was then performed with consecutive injections of inhibitors of the electron transport chain: 1 µM oligomycin, 1 µM FCCP (Carbonyl cyanide-4-(trifluoromethoxy) phenylhydrazone), and a mix of 0.5 µM rotenone / 0.5 µM antimycin A. OCR (oxygen consumption rate) and ECAR (extracellular acidification rate) were measured and then normalized according to protein content. The individual parameters (basal respiration, maximal respiration, spare respiratory capacity, mitochondrial ATP production and proton leak) were all determined by calculating the area under the curves using the Seahorse Wave Desktop Software, as previously described by Dranka *et al.* (2011). Five independent experiments were performed.

2.12- Triglyceride and free fatty acid measurement

Extraction of total lipids from cells was first performed according to the Folch method. Total lipids dissolved in ethanol were then used for triglyceride measurement with the LabAssay™ Triglyceride Kit (Wako Chemicals GmbH, Neuss, Germany); measurement of free fatty acids was

realized using the NEFA-HR kit (Wako Chemicals GmbH, Neuss, Germany). The manufacturer's protocols were applied for both kits. A Spectrostar Nano microplate reader (BMG Labtech, Ortenberg, Germany) was used to monitor the absorbance.

2.13- Statistical analysis

All values were presented as means ± Standard Deviation from a minimum of three independent experiments. Statistical analyses were performed using one-way analysis of variance ANOVA followed by a Student-Newman-Keuls post-test. All statistical analyses were assessed using GraphPad Prism5 software (San Diego, United States). Significance was accepted at $p<0.05$.

3-RESULTS

3.1. Co-exposing steatotic WIF-B9 hepatocytes to MEHP and ethanol enhances cell death, notably *via* activation of effector caspases and p53 pathway

The first set of experiments was carried out in order to test the impact of MEHP/ethanol co-exposure on the death of WIF-B9 hepatocytes in the presence or not of a prior steatosis. To do so, the concentration of MEHP was set at 500 nM, based upon a viability assay (MTT test), showing no significant cell viability loss at this concentration in non-steatotic hepatocytes (Supplementary Fig. S2A). Regarding ethanol, the test concentration was set at 5 mM, *i.e.* a sub-toxic concentration, as previously reported (Bucher *et al.*, 2018b). Following 5 days of treatment by either toxicant alone or in combination, the number of apoptotic and necrotic cells was evaluated using Hoechst 33342 and Sytox green staining, respectively. As illustrated in Fig. 1A and B, the number of both apoptotic and necrotic cells was significantly increased in all steatotic cells compared to non-steatotic counterparts. However, the most striking effect was observed upon co-exposing steatotic cells to MEHP and ethanol (ME), especially concerning apoptosis, with a 2-fold increase compared to steatotic control (C) cells (Fig. 1A). A significant increase in necrosis was also observed with MEHP/ethanol co-exposure under steatotic conditions compared to steatotic controls; however it was similar to that induced by MEHP alone. In order to further characterize the type of cell death involved, and as caspase activation was previously shown to play a role in the toxicity of MEHP in liver cells (Yang *et al*., 2015), the broad caspase inhibitor zVAD (10 µM) was used to evaluate the possible role of effector caspases. Fig.1C shows that following zVAD treatment, the number of cells with condensed/fragmented chromatin was significantly reduced under co-exposure conditions as well as upon treatment with MEHP alone. Furthermore, an increase in caspase activity was detected upon treatments with either MEHP/ethanol or MEHP alone (Fig. 1D), but without any significant difference between these two conditions; this was associated with an increase in cleaved caspase-3 under both conditions (Fig.1E). Note that co-exposure significantly decreased cell proliferation, but no difference was detected between steatotic and non steatotic cells (Supplementary Fig. S2B). Moreover, no change in the regulation of gene

expression related to inflammation was observed under our experimental conditions (Supplementary Fig. S3).

As MEHP was previously shown to induce DNA damage related to apoptosis in normal human liver cell line L02 (Yang *et al*., 2015), we then tested the appearance of such a phenomenon; to do so, an analysis of γ-H2AX staining was performed (see *eg.* Tête *et al*., 2018). As shown in Fig. 2A, a significant increase in DNA damage occurred in steatotic cells co-exposed to MEHP and ethanol as compared to steatotic control cells. Such DNA damage was confirmed when looking at the 53BP1 foci (*i.e.* a key regulator of Double Strand Break repair), whose area relative to nucleus was significantly enhanced upon co-exposure (Supplementary Fig. S4A and C); such an increase was also validated by western blotting (insert, supplementary Fig. S4A). Based upon the fact that an activation of the tumor suppressor protein p53 was previously shown to be related to MEHP-induced DNA damage and subsequent cell death (Yang *et al*., 2015), we next decided to test the involvement of the p53 pathway under steatotic conditions. The effect of pifithrin-α (PFT; 10 µM), known to inhibit p53 activation, was then tested. As illustrated in Fig. 2B, PFT significantly reduced, though not fully, the number of apoptotic cells induced by MEHP/ethanol co-exposure or MEHP alone in presence of steatosis. We next looked for p53 activation by immunochemistry. Data from Fig.2C and D clearly pointed to an increase in the nuclear p53 staining both upon MEHP alone and MEHP/ethanol co-exposure of steatotic cells; this was confirmed by western blotting indicating an increase in the phosphorylation state of p53 upon MEHP and co-exposure (Fig. 2E). This p53 activation upon co-exposure was paralleled by an induction (although not significant) by ~50% of the *gadd45* mRNA expression, with less effect on *p21*, that is, two well-known gene targets of p53 (Supplementary Fig. S5) (Liamin *et al*., 2017). It is also worth emphasizing that co-exposure did not significantly change the parameters of mitochondrial respiration (Supplementary Fig.S6), nor cell metabolic phenotype (Supplementary Fig.S7) under steatotic conditions. Likewise, the free fatty acid content of steatotic cells remained unchanged upon co-exposure (Supplementary Fig. S8A), and also no change in triglyceride content was observed (Supplementary Fig. S8B). These data therefore ruled out mitotoxicity and lipotoxicity as possible causes of the apoptosis induced by co-exposure under our experimental conditions.

Altogether, these first results demonstrated that the cell death induced by co-exposing steatotic WIF-B9 hepatocytes to MEHP and ethanol involved, at least in part, a caspase-dependent apoptotic pathway, that might result from a p53 activation triggered by DNA damage.

3.2. Involvement of ADH in the cell death induced by co-exposing steatotic WIF-B9 hepatocytes to MEHP and ethanol

We next tested the involvement of ethanol metabolism in the toxicity induced by co-exposure of steatotic cells, by using 4-methyl pyrazole (4-MP; 500 µM), a known inhibitor of both CYP2E1 and alcohol dehydrogenase (ADH; Cornell *et al*., 1983; Swaminathan *et al*., 2013). As shown in Fig. 3A, 4-MP significantly inhibited the cell death induced by MEHP/ethanol co-exposure in steatotic cells. This therefore highlighted a role for ethanol metabolism in the toxicity induced by co-exposure under steatotic conditions.

The activity of CYP2E1 was then analyzed following 5 days of co-exposure to MEHP and ethanol, as an activation of this CYP has been previously suggested to be involved in steatosis progression (Aubert *et al*., 2011). We found that this activity was rather significantly reduced in steatotic cells whatever the condition tested (Fig. 3B). As 4-MP can also inhibit ADH, the major enzyme system for metabolizing alcohol especially at low concentrations (Cederbaum, 2012; Crabb *et al.*, 1987), the activity of this enzyme was next studied (Fig. 3C). ADH activity was measured following 3 h of treatment based upon the fact that it is not increased following chronic alcohol consumption (Crabb *et al*., 1987). We found that ADH activity was significantly enhanced by co-exposure to MEHP and ethanol of steatotic cells, whereas no effect of MEHP or ethanol alone was detected (Fig. 3C). Note that no significant change in the mRNA expression of several ADH isoforms could be detected at that time under steatotic conditions (Fig. 3D). Knowing that AhR (aryl hydrocarbon receptor) was previously suggested to play a role in the regulation of liver ADH activity (Tête *et al*., 2018), we decided to test the effect of CH-223191 (CH; 3 µM), an AhR specific antagonist, on ADH activity as well as DNA damage and cell death. Our data clearly showed that this AhR antagonist prevented not only the early increase in ADH activity elicited by co-exposing steatotic cells to both MEHP and ethanol for 3 h (Fig. 4A), but also the related DNA damage (Fig. 4B) and

apoptosis induced after 5 days of treatment (Fig. 4C). Similar results regarding cell death were also obtained with another known AhR antagonist, *i.e*. α-naphthoflavone (αNF, 10 µM; Fig. 3C). Note that AhR antagonism by CH or αNF also prevented DNA damage and/or cell death induced by MEHP alone.

Altogether, these results therefore pointed to a role for an AhR-dependent ADH activation, in the toxic effects of the co-exposure to MEHP/ethanol under steatotic conditions.

3.3. Involvement of CYP4A in the cell death induced by co-exposing steatotic WIF-B9 hepatocytes to MEHP and ethanol

It has previously been reported that cytochrome P450 4A (CYP4A) could play an important role in the development of steatosis as well as in its progression towards steatohepatitis, notably *via* oxidative stress (Park *et al*., 2014; Ryu *et al*., 2019; Zhang *et al*., 2017a). Knowing that phthalates, especially MEHP, can induce the expression of those CYPs (Bell and Elcombe, 1991), notably through PPAR activation (Xu *et al*., 2008), we next tested a possible involvement of CYP4s in the increase in the cell death induced by MEHP/ethanol co-exposure under steatotic conditions. First, the mRNA expression of several CYP4A isoforms (1 to 3) was evaluated (Figs 5A-C). As expected from previous work (Park *et al*., 2014; Ryu *et al*., 2019), this expression was found to be up-regulated upon steatosis, whatever the isoform tested. Regarding the impact of treatments, whereas a trend towards a further up-regulation could be observed with all treatments compared to steatotic controls, no significant difference appeared, likely due to rather large standard deviations. However, especially for CYP4A2 and 3, a 2-fold increase would be triggered by MEHP/ethanol co-exposure (Figs 5B and C). Regarding CYP4A protein level (Fig. 5D and supplementary Fig. S9A), no further increase upon treatments could be detected when compared to steatotic controls, as confirmed by the densitometric analysis. Note that inhibiting AhR by CH did not affect the increase in CYP4A protein level induced by steatosis (supplementary Fig. S9A), and a rather similar mRNA expression of *Pparα*, a known regulator of CYP4A expression (Ito *et al*., 2006), was observed whatever the condition tested (supplementary Fig. S9B).

To evaluate a possible role for CYP4A activity in co-exposure-induced cell death, we used HET0016 (500 nM), a known inhibitor of these CYPs (Park *et al*., 2014; Seki *et al*., 2005). As shown in Fig. 5E, the increased number of apoptotic cells due to MEHP/ethanol co-exposure under steatotic conditions was fully inhibited. A similar inhibition was also observed upon MEHP treatment. Such an inhibition was paralleled by a prevention of the co-exposure-related DNA damage (Fig. 5F).

Taken together, our data indicated a role for CYP4A activity in the toxic effects of the co-exposure to MEHP/ethanol under steatotic conditions.

3.4. Involvement of oxidative stress in the cell death induced by co-exposing steatotic WIF-B9 hepatocytes to MEHP and ethanol

In order to get further insight into the intracellular mechanisms involved in the toxic effects of MEHP/ethanol co-exposure in steatotic hepatocytes, we tested a possible role for reactive oxygen species (ROS). Indeed, ROS production, *via* the induction of oxidative stress, is well recognized as a "second hit" for the pathological progression of NAFLD (see *eg.* Engin, 2017 and Spahis *et al*., 2017, for reviews). Besides, they have previously been shown to be involved in the cell death induced by B[*a*]P/ethanol co-exposure in steatotic cells (Bucher *et al*., 2018a; Tête *et al*., 2018), and both ethanol and MEHP metabolisms are known to induce oxidative stress (Kurose *et al*., 1996; Liu *et al*., 2017; Park *et al*., 2020; Sergent *et al*., 2005). Using co-treatment with thiourea (6.25 mM; a scavenger of hydroxyl radicals, superoxide anion and hydrogen peroxide; Farmer *et al*., 2006, Kelner *et al*., 1990), we first found that cell death (Fig. 6A) induced by co-exposing steatotic cells to MEHP and ethanol was significantly blocked, thus suggesting a role for ROS in this toxicity; the effects of MEHP alone were also prevented. In order to test the occurrence of an oxidative stress, oxidative damage was next searched, notably with regard to DNA damage. Thus, using the co-treatment with thiourea, we found that the DNA damage induced by co-exposing steatotic cells to MEHP and ethanol was fully inhibited, thus pointing to DNA oxidation (Fig. 6B). Such a result was also suggested by immunolocalization data obtained with an antibody against 8-oxo-Guanine (8-oxoG; one of the most common DNA lesions resulting from ROS modifying guanine), even though these results would deserve further validation, due to large variability (Supplementary Fig. S4B and C). In addition to possible DNA

oxidation, we also observed a trend towards an increased MDA concentration, that is, a sign of lipid peroxidation (Fig. 6C), thus confirming the occurrence of oxidative stress upon MEHP/ethanol co-expsoure. It is worth noting that, whereas MEHP significantly increased the superoxide anion production, it was not the case for co-exposure (Fig. 6D). As for B[a]P/ethanol co-exposure (Tête *et al*., 2018), one might then suppose a role for NO and hence peroxynitrite formation to induce oxidative damages.

Altogether, these results therefore demonstrated a role for oxidative stress in the cell death induced by co-exposing steatotic cells to MEHP and ethanol.

3.5. Co-exposure to DEHP and ethanol also elicits liver damage *in vivo* in HFD zebrafish larvae

Having shown that *in vitro* co-exposure to MEHP and ethanol can induce death of steatotic hepatocytes, we next tested whether DEHP, whose MEHP is the primary intermediate metabolite (Thomas *et al*., 1982; Wang *et al*., 2019), in combination with ethanol, could lead *in vivo* to a pathological progression of steatosis. To this aim, we used an *in vivo* zebrafish larvae model fed a high fat diet (HFD), that we previously used to test the impact of a co-exposure to B[*a*]P and ethanol (Bucher *et al*., 2018b; Imran *et al*., 2018). Following the onset of steatosis, larvae were exposed for 7 days to co-exposure or either molecule alone (Supplementary Fig. S1B), at concentrations shown to be non-toxic in larvae fed with a standard diet (SD): ethanol, 43 mM (see Bucher *et al*., 2018b; Imran *et al*., 2018); DEHP, 2.56 nM (supplementary Fig. S10; as no significant loss in larvae viability was observed even at 2.56 µM, the test concentration was chosen based on human oral exposure [1 to 10 nM]; ATSDR, 2019). In order to evaluate liver toxicity, a histological analysis was performed. We found that HFD markedly increased DEHP/ethanol co-exposure toxicity (Fig. 7A), with the appearance of ballooning and vacuolized hepatocytes as well as cellular dropouts (see Imran *et al*., 2018, for typical figures). To further validate such effects, the mRNA expression of genes previously shown to be related to hepatotoxicity, namely *zgc163022*, *tfa*, *tgfb* and *casp3* (Imran *et al*., 2018), was

analyzed. As shown in Figs 7B-E, a trend towards an up-regulation was observed, with a significant effect regarding *tfa*, when compared to HFD control larvae (Fig. 7C). Despite the fact that we did not see any sign of inflammation in *in vitro* experiments (supplementary Fig. S3), we decided to look for such a phenomenon *in vivo*. To do so, the mRNA expression of several genes linked to inflammation was tested: *il1b*, *crp*, *cp* and *nfkb* (Fig. 8). Whereas a trend towards an up-regulation of the two former genes was observed upon DEHP/ethanol co-exposure in HFD larvae (Figs 8A and B), a significant induction occurred for *cp* (ceruloplasmin gene; Fig. 8C) and *nfkb* (Fig. 8D).

Altogether these results suggested that DEHP/ethanol co-exposure increased liver toxicity in HFD larvae, and that this was associated with a regulation of gene expression related to inflammation. It is worth noting that a significant increase in the mRNA expression of *AhR* and *cyp4t8* (*i.e.* the homolog gene of mammal *CYP4A*) was detected (Supplementary Fig S11B and D).

4-DISCUSSION

The progression of liver steatosis has previously been suggested as partly relying on exposure to environmental contaminants (Foulds *et al*., 2017; Heindel *et al*., 2017; Wahlang *et al*., 2019). In line with this, our previous work has demonstrated, both *in vitro* and *in vivo*, that co-exposure to the known carcinogen, B[*a*]P, and the lifestyle factor, ethanol, can favor the death of hepatocytes as well as the onset of inflammation in presence of prior steatosis (Bucher *et al*., 2018b; Imran *et al*., 2018; Tête *et al*., 2018). The present study further emphasizes the fact that, on a background of liver steatosis (1st hit), chronic co-exposure to multiple risk factors (2nd hit) could promote the development of steatohepatitis. Indeed, our data show an increase in the death of steatotic hepatocytes when co-exposed to ethanol and phthalates (DEHP or its main metabolite MEHP) both *in vivo* and *in vitro,* respectively. In addition, early signs of inflammation were detected in co-exposed-HFD zebrafish larvae, thus supporting the progression of steatosis towards a steatohepatitis-like state.

DEHP is a well-known obesogen, due to its impact on homeostatic metabolic pathways (Grün, 2010), thereby participating in the development of liver steatosis (Foulds *et al*., 2017). Nevertheless, to our knowledge, only one study has shown that this pollutant can exacerbate NAFLD in rats fed a high-fat diet, especially when HFD animals received by gavage a daily dose of 500 mg/kg of DEHP for 8 weeks (Chen *et al*., 2016). Indeed, the authors found an increase in serum aspartate aminotransferase (AST) and alanine aminotransferase (ALT) activities as well as an increase in the serum content of the cytokines TNFα and IL6. In the present study, HFD zebrafish larvae were exposed to an environmentally realistic dose of DEHP (2.56 nM in bath water, that is, ~1 ng/mL) for 7 days; note that human oral exposure has been reported to range from 3 to 30 µg/kg/day (ATSDR, 2019). Besides, in pregnant women, the mean DEHP concentrations detected in maternal and cord plasmas were 1.15 ± 0.81 and 2.05 ± 1.47 µg/mL, respectively; and the mean MEHP concentrations 0.68 ± 0.85 and 0.68 ± 1.03 µg/mL, respectively (Latini *et al.*, 2003). DEHP alone did not appear to induce liver toxicity under our conditions (Fig. 7), as evaluated by histology analysis or expression of genes previously related to hepatotoxicity (Imran *et al*., 2018). In contrast, when combined to 43 mM ethanol (corresponding to an internal dose of 10 mM; data not shown), this pollutant led to hepatotoxicity, and

a significant increase in ceruloplasmin (*cp*) gene expression was detected. This protein, known to be mainly produced by liver, acts as an acute phase reactant in inflammation and tissue damage (Gitlin, 1988). Regarding the other inflammation markers tested, *i.e.* interleukin-1β and C-reactive protein (CRP), the observation of a trend towards increase upon co-exposure, though not significant, might indicate further exacerbation of the inflammation with longer time treatments. The fact that DEHP, when given orally, is first metabolized into MEHP notably by intestinal lipases (Albro and Lavenhar, 1989), prompted us to test the impact of this metabolite on steatotic WIF-B9 hepatocytes in order to elucidate the intracellular mechanisms underlying the toxicity of co-exposure. An increase in cell death, especially apoptosis, was observed with MEHP (500 nM, 5 days-treatment) alone, but only in presence of steatosis; this was further exacerbated when combined to a low dose (5 mM) of ethanol, thus mimicking the *in vivo* effects. Note that the MEHP concentration of 500 nM (≈ 0.2 µg/mL) was in the same range as the MEHP concentrations measured in maternal and cord plasma samples (Latini *et al.*, 2003). However, in contrast to what was observed with the *in vitro* effects of B[*a*]P/ethanol co-exposure showing changes in the expression of several genes related to inflammation (Bucher *et al*., 2018b), no such changes were detected after 5 days of treatment. The difference between both types of co-exposure might be due to different xenosensor activities (*eg*. AhR, CAR, PPARα) and/or intracellular signaling pathways triggered by B[*a*]P and MEHP (Foulds *et al*., 2017; Wahlang *et al*., 2019).

Regarding the type of cell death induced by the MEHP/ethanol co-exposure under steatotic conditions, our data showed that it was apoptosis partly involving a p53 and a caspase-dependent pathway, likely resulting from an oxidative DNA damage. This was also the case regarding MEHP alone. It is worth noting that in non-steatotic liver cells HepG2 and L02, MEHP has been reported to activate a DNA damage-related p53 apoptotic pathway, but the effective concentrations in these studies were over 10 µM (Yang *et al*., 2012, 2015; Chen *et al.*, 2012), compared to 500 nM used in the present study. Interestingly, in CHO AS52 cells lacking Base Excision Repair (BER) system, a 1 mM concentration of MEHP was found to cause DNA-single strand breaks at a level similar to that found in regular AS52 cells exposed to 25 mM of MEHP (Chang *et al*., 2017). In this context, it would be

interesting to evaluate the BER pathway under co-exposure to MEHP/ethanol in steatotic WIF-B9 cells. Indeed, a negative impact of steatosis on cell DNA damage repair capacity might explain why cell proliferation was similarly impacted by MEHP/ethanol in both steatotic and non-steatotic cells (supplementary Fig. S2B), whereas only a small increase in cell death was detected in these latter cells compared to the former ones (Fig. 1A). In line with this, Gao and coworkers (2004) have previously demonstrated an inverse relationship between oxidative DNA damage and DNA repair enzyme expression (especially the MYH DNA glycosylase) in different murine models of fatty liver disease. Regarding the possible apoptotic mechanisms involved, it has previously been shown that in MEHP-exposed HepG2 cells, the p53-dependent apoptosis was related to an enhanced protein level of the Bax/Bcl-2 ratio, thus supporting a role for a mitochondrial intrinsic pathway (Chen *et al*., 2012). Similar effects, along with a decreased Bcl-XL protein content, another anti-apoptotic member of the Bcl-2 family, were also observed in the rat liver cell line BRL treated with 200 µM DEHP (Ha *et al*., 2016). Moreover, an increased Bax (pro-apoptotic) and decreased Bcl-2 (anti-apoptotic) mRNA expression was reported for MEHP-induced apoptosis in human monocytic leukemia U937 cells (Yokoyama *et al.*, 2003), and a transcriptional regulation by p53 of these proteins was proposed. Here, no significant change in Bax and Bcl-2 mRNA expression was observed upon MEHP/ethanol co-exposure, and so for Bcl-XL (supplementary Fig. S12). As NOXA and PUMA, two known BH3 domain-only proteins of Bcl-2 family regulated by p53, were previously reported to be up-regulated by MEHP in HepG2 cells (Yang *et al*., 2012), their expression would be worth testing in steatotic WIF-B9 hepatocytes co-exposed to MEHP and ethanol.

We have previously shown that co-exposing steatotic human HepaRG hepatocytes to B[*a*]P and ethanol led to AhR-dependent alterations of mitochondrial function. Indeed, reductions in mitochondrial respiratory chain activity, mitochondrial respiration, and mitochondrial DNA levels were detected in relationship with a ROS overproduction (Bucher *et al*., 2018a). In addition, it has been shown that: (1)-MEHP (100 µM) can alter the function of isolated rat liver mitochondria, notably by acting as an uncoupling agent and an inhibitor of the succinate dehydrogenase activity (Melnick and Schiller, 1982); and (2)-chronic alcohol intake impaired hepatic mitochondrial oxidative

phosphorylation (García-Ruiz and Fernández-Checa, 2018). In this context, the impact of MEHP/ethanol co-exposure was tested on the mitochondrial respiration in steatotic WIF-B9 hepatocytes. Whatever the parameter evaluated, no significant change was detected (supplementary Fig. S6), and the metabolic phenotype remained quite similar in treated *versus* untreated steatotic hepatocytes (supplementary Fig. S7). A trend towards a "stressed" metabolic phenotype (as visualized by an increased OXPHOS and glycolysis), was nevertheless seen upon cell treatment with a highest test MEHP concentration (10 µM for 5 days). A role for mitochondrial dysfunction is claimed to be a general characteristic in the exacerbation of steatosis (García-Ruiz and Fernández-Checa, 2018), so that NASH has been considered as a mitochondrial disease (Pessayre and Fromenty, 2005). However, this concept has been thereafter challenged by experimental data indicating that a moderate decreased mitochondrial respiration would prevent rather than promote steatohepatitis (Pospisilik *et al*., 2007). In this context, the fact that no alteration in mitochondrial oxygen consumption was observed upon MEHP/ethanol co-exposure despite the occurrence of an oxidative stress-dependent cell death might fit with the notion that the decrease in mitochondrial respiration would not be the triggering event underlying the transition of steatosis towards a more severe state. Considering that point, our data thus favor the hypothesis that the altered mitochondrial respiration usually related to the development of steatohepatitis would be a long-term consequence rather than a cause, likely resulting from oxidative stress.

Regarding the induction of oxidative stress under our experimental conditions, as DEHP has previously been reported to be able to localize in bovine heart muscle mitochondria (Nazir *et al*., 1971), one might propose that MEHP would also have this capacity, thereby favoring the generation of pro-oxidant species ($O_2^{\cdot-}$/H_2O_2). Such a mitochondrial oxidative stress without disruption of OXPHOS has recently been observed with MitoPQ (mitochondria-targeted paraquat) in adipocytes (Fazakerley *et al*., 2018). Another source of oxidative stress during NAFLD progression could relate to CYP2E1 activation by ethanol. Indeed, a higher hepatic CYP2E1 expression and activity has been reported in the context of obesity and NAFLD (Aubert *et al*., 2011). In addition, such an increase has been found to lead to ROS production during metabolism of ethanol, and even in the absence of any

substrate *via* incomplete reduction of oxygen (Cederbaum, 2010; Lieber, 2004; Lu and Cederbaum, 2008). However, this hypothesis can be ruled out under our experimental conditions since a decrease rather than an increase in CYP2E1 activity was observed, even in the presence of ethanol (Fig. 3B). Note that no change in the *cyp2y3* expression (*CYP2E1* gene homolog in zebrafish; supplementary Fig.S11A) was observed in our *in vivo* experiments. Such an absence of CYP2E1 activation has previously been observed in steatotic hepatocytes (HepaRG or WIF-B9) upon B[*a*]P/ethanol co-exposure (Bucher *et al*., 2018a; Tête *et al*., 2018). Interestingly, it has been reported that repeated oral administration of DEHP in rats accelerates the clearance of ethanol from blood due to an increase in the activity of ADH (Agarwal *et al*., 1982). Furthermore, the *in vivo* effects of orally administered DEHP on ADH activity appeared to be reproduced upon MEHP exposure (Lake *et al*., 1975). Since 4-MP (a known inhibitor of CYP2E1 and ADH) inhibited the cell death induced by MEHP/ethanol co-exposure despite the decrease in CYP2E1 activity, ADH activity was naturally analyzed; besides, the primary pathway of ethanol metabolism in liver is known to involve this enzyme (Thurman and McKenna, 1975). Similarly to what was previously observed with the B[*a*]P/ethanol co-exposure (Tête *et al*., 2018), we found here that MEHP/ethanol co-exposure, but not the chemicals alone, also induced an early (3h) increase in ADH activity. Under these conditions, one can thus expect an enhanced metabolism of ethanol. Of note, one consequence of the reaction of ethanol with ADH is ROS production, *via* fueling NADH to mitochondria (Bailey and Cunningham, 1998). Regarding the origin of this activation, it seems that it is not due to a change in the mRNA expression of different ADH isoforms (Fig. 3D). Surprisingly, using a specific AhR antagonist, we found that this cytosolic receptor might be involved in the early increase in ADH activity (Fig. 4B), as previously reported for the B[*a*]P/ethanol co-exposure (Tête *et al*., 2018). Interestingly, it has previously been shown that phthalates can rapidly activate AhR either through non-genomic (Tsai *et al*., 2014) or genomic (Rusyn and Corton, 2012; Wójtowicz *et al*., 2017) pathways. The fact that no increase in AhR expression nor in CYP1A1 expression or activity, was observed upon MEHP/ethanol co-exposure (supplementary Fig. S13), might favor a non-genomic pathway. Another possible source of ROS upon MEHP/ethanol co-exposure might be NADPH oxidase. Indeed, activation of this enzyme has been previously found to favor the NAFLD progression in HFD mice (García-Ruiz *et al*., 2016). In line with this, it is

noteworthy that an activation of NADPH oxidase could be detected under co-exposure, as visualized by an increase in the serine phosphorylation of $p47^{phox}$ (supplementary Fig. S14; Reinher *et al*., 2005). Despite oxidative damages (on DNA and lipids), the fact that no further increase (rather a decrease) in superoxide anion was observed upon co-exposure as compared to MEHP alone (Fig. 6D) would favor the hypothesis of a role for NO and peroxynitrite in such damages, as previously observed upon B[a]P/ethanol co-exposure (Tête et al., 2018).

In addition to the role of ADH in the observed toxicity, our results obtained with HET0016 also point to an implication of CYP4A activity in the DNA damage and related cell death induced by MEHP/ethanol co-exposure; similar results were also obtained with MEHP alone. Whereas CYP4A has already been shown to play a role in the development of hepatic steatosis and its progression (Park *et al*., 2014; Ryu *et al*., 2019; Zhang *et al*., 2017a), to our knowledge, the present study is the first one describing a role for this CYP in the progression of steatosis upon exposure to environmental chemicals. The CYP4 family catalyzes omega-hydroxylation of saturated, branched chain, and unsaturated fatty acids (Simpson, 1997; Hardwick, 2008), but has also been shown to be involved in phthalate metabolism (Choi *et al*., 2012). In line with this, an increase in the activity of CYP4A1 has been reported in the liver of rats exposed to DEHP or MEHP (Dirven *et al*., 1992). An induction of CYP4A expression has also been found in the liver of rodents with genetically induced- or diet-induced diabetes, both models exhibiting liver steatosis (Vornoli *et al*., 2014). Here, a significant increase in both mRNA expression and protein level of CYP4A was detected in control steatotic WIF-B9 hepatocytes compared to non steatotic counterparts; although not significant, a trend towards a 2 fold-induction of CYP4A mRNA expression was observed upon MEHP/ethanol co-exposure, but without any change in CYP4A protein level. Regarding our *in vivo* model, co-exposure to DEHP and ethanol also up-regulated the *Cyp4t8* mRNA expression in HFD zebrafish larvae (supplementary Fig. S11B). In this latter case, it is noteworthy that the mRNA expression of *ppara* and *pparb* also tends to increase (supplementary Fig. S11E and F), knowing that these nuclear receptors are involved in the regulation of CYP4A expression (Bell and Elcombe, 1991; Hardwick *et al*., 2009; Ip *et al*., 2003). Note also that a study previously reported an impact of MEHP (30 µM) on DNA methylation in

Zebrafish embryos, with consequences on adipogenesis pathway, especially in link with PPAR regulation (Kamstra et al., 2017). Thus, it would be worth analyzing in the future epigenetic alterations under MEHP/ethanol co-exposure. With respect to the role for CYP4A in toxicity, Park and co-workers (2014) have found that its inhibition by HET0016 or using a shRNA strategy in diabetic mice prevented hepatic ER stress, insulin resistance and apoptosis; similar results have recently been obtained in a novel 3D hepatic steatosis model (Ryu *et al*., 2019). Such an involvement of CYP4A in ER stress and related cell death would involve microsomal oxidative stress related to NAFLD, as previously suggested (Leclercq *et al*., 2000). In this latter study, CYP4A enzymes were found to work as alternative catalysts for oxidative stress in the absence of CYP2E1. A similar pattern, *i.e.* a high CYP4A and low CYP2E1 expression, was observed in our study. In this context, CYP4A activity under our experimental conditions might play a role in co-exposure toxicity through the induction of oxidative damage. This is notably supported by our findings that both HET0016 and the antioxidant thiourea prevented the increase in DNA damage induced by MEHP/ethanol co-exposure. Considering the mechanisms described above, several pathways might thus be responsible for the oxidative stress induced by the co-exposure in steatotic hepatocytes.

5-CONCLUSION

The present study indicates that co-exposing steatotic hepatocytes to both MEHP and ethanol can lead to cell death, at least partly through activation of a p53- and caspase-dependent apoptotic process likely stemming from oxidative DNA damage (Fig. 9). Such an increase in hepatotoxicity also occurs *in vivo* in HFD-fed zebrafish larvae co-exposed to DEHP and ethanol alongside an up-regulation of gene expression related to inflammation, thereby pointing to NAFLD exacerbation. Cooperative mechanistic interactions between MEHP and ethanol appear essential, notably *via* an increase in ethanol metabolism by ADH, possibly depending on AhR activation by the phthalate, and *via* CYP4A activation, possibly involved in oxidative stress. Based upon the present data and previous work (Tête *et al*., 2018), it therefore seems that AhR, *via* an early ADH activation, might be a key

determinant in enhancing ethanol metabolism leading to the pathological progression of steatosis upon co-exposure to environmental pollutant and ethanol. In order to firmly validate this hypothesis, it will be interesting to test the effects of co-exposing steatotic hepatocytes to ethanol and other AhR-activating pollutants.

CREDIT AUTHORSHIP CONTRIBUTION STATEMENT

Arnaud Tête: Investigation, Formal analysis, Visualization, Writing - original draft ; **Isabelle Gallais**, **Muhammad Imran** : Investigation, Formal analysis, Visualization, Writing - review & editing; **Corinne Martin-Chouly, Lydie Sparfel**: Methodology, Writing - review & editing ; **Louis Legoff, Maëlle Bescher**: Investigation; **Odile Sergent** : Conceptualization, Methodology, Writing - review & editing, Supervision ; **Normand Podechard** : Conceptualization, Methodology, Formal analysis, Funding acquisition, Supervision; **Dominique Lagadic-Gossmann**: Conceptualization, Formal analysis, Visualization, Writing - original draft, Writing - review & editing, Funding acquisition, Supervision, Project administration.

DECLARATION OF COMPETING INTEREST

The authors declare that they have no known competing financial interests or personal relationships that could have appeared to influence the work reported in this paper.

ACKNOWLEDGEMENTS

We wish to thank the MRic (Microscopy-Rennes Imaging Center) and H2P2 (Histopathology High precision) facilities (SFR Biosit, Université de Rennes 1) for, respectively, microscopy and histology experiments, especially Stéphanie Dutertre and Alain Fautrel for their technical assistance. We are also very grateful to INRA, LPGP (Institut National de la Recherche Agronomique, Laboratoire de Physiologie et Génomique des Poissons, Rennes) for providing zebrafish eggs. We wish to thank Doris Cassio for providing the WIF-B9 cell line. This work would not have been possible without the fruitful scientific discussions with Drs Marie-Anne Robin, Bernard Fromenty and Fatima Smagulova, and without the technical input of Martine Chevanne, Marie Liamin and Dimitri Gobart. AT was a recipient of a fellowship from the Région Bretagne (ARED) and the Agence Nationale de la Recherche (ANR). We also wish to thank the faculty of Pharmacy (Université de Rennes) for awarding a 2-month fellowship to AT. M.I. was a recipient of a fellowship from the Higher Education Commission, Pakistan. This work was supported by ANR [STEATOX project: “ANR-13-CESA-0009”], as well as by ANSES (Z-MENACE project: N° 2019/1/128).

APPENDIX A. Supplementary information (including figures and tables)

REFERENCES

Agarwal DK, Agarwal S, Seth PK. Interaction of di-(2-ethylhexyl) phthalate with the pharmacological response and metabolic aspects of ethanol in mice. Biochem Pharmacol. 1982 Nov 1;31(21):3419-23.

Albro PW, Lavenhar SR. Metabolism of di(2-ethylhexyl)phthalate. Drug Metab Rev. 1989;21(1):13-34.

Al-Eryani L, Wahlang B, Falkner KC, Guardiola JJ, Clair HB, Prough RA, Cave M. Identification of Environmental Chemicals Associated with the Development of Toxicant associated Fatty Liver Disease in Rodents. Toxicol Pathol. 2015 Jun;43(4):482-97. doi: 10.1177/0192623314549960

ATSDR, Agency for Toxic Substances and Disease Registry. 2019. Toxicological profile for Di(2-ethylhexyl)phthalate (DEHP). Atlanta, GA: U.S. Department of Health and Human Services, Public Health Service.

Aubert J, Begriche K, Knockaert L, Robin MA, Fromenty B. Increased expression of cytochrome P450 2E1 in nonalcoholic fatty liver disease: mechanisms and pathophysiological role. Clin Res Hepatol Gastroenterol. 2011 Oct;35(10):630-7. doi: 10.1016/j.clinre.2011.04.015.

Bai J, He Z, Li Y, Jiang X, Yu H, Tan Q. Mono-2-ethylhexyl phthalate induces the expression of genes involved in fatty acid synthesis in HepG2 cells. Environ Toxicol Pharmacol. 2019 Jul;69:104-111. doi: 10.1016/j.etap.2019.04.004

Bailey SM, Cunningham CC. Acute and chronic ethanol increases reactive oxygen species generation and decreases viability in fresh, isolated rat hepatocytes. Hepatology. 1998 Nov;28(5):1318-26.

Bell DR, Elcombe CR. Induction of acyl-CoA oxidase and cytochrome P450IVA1 RNA in rat primary hepatocyte culture by peroxisome proliferators. Biochem J. 1991 Nov 15;280 (Pt 1):249-53.

Benjamin S, Masai E, Kamimura N, Takahashi K, Anderson RC, Faisal PA. Phthalates impact human health: Epidemiological evidences and plausible mechanism of action. J Hazard Mater. 2017 Oct 15;340:360-383. doi: 10.1016/j.jhazmat.2017.06.036

Bucher S, Le Guillou D, Allard J, Pinon G, Begriche K, Tête A, Sergent O, Lagadic-Gossmann D, Fromenty B. Possible Involvement of Mitochondrial Dysfunction and Oxidative Stress in a Cellular Model of NAFLD Progression Induced by Benzo[*a*]pyrene/Ethanol CoExposure. Oxid Med Cell Longev. 2018a Jul 26;2018:4396403. doi: 10.1155/2018/4396403

Bucher S, Tête A, Podechard N, Liamin M, Le Guillou D, Chevanne M, Coulouarn C, Imran M, Gallais I, Fernier M, Hamdaoui Q, Robin MA, Sergent O, Fromenty B, Lagadic-Gossmann D. Co-

exposure to benzo[a]pyrene and ethanol induces a pathological progression of liver steatosis in vitro and in vivo. Sci Rep. 2018b Apr 13;8(1):5963. doi: 10.1038/s41598-018-24403-1

Cederbaum AI. Role of CYP2E1 in ethanol-induced oxidant stress, fatty liver and hepatotoxicity. Dig Dis. 2010;28(6):802-11. doi: 10.1159/000324289

Cederbaum AI. Alcohol metabolism, Clin. Liver Dis. 2012; 16:667-685. doi: 10.1016/j.cld.2012.08.002

Chalasani N, Younossi Z, Lavine JE, Charlton M, Cusi K, Rinella M, Harrison SA, Brunt EM, Sanyal AJ. The diagnosis and management of nonalcoholic fatty liver disease: Practice guidance from the American Association for the Study of Liver Diseases. Hepatology. 2018 Jan;67(1):328-357. doi: 10.1002/hep.29367

Chang YJ, Tseng CY, Lin PY, Chuang YC, Chao MW. Acute exposure to DEHP metabolite, MEHP cause genotoxicity, mutagenesis and carcinogenicity in mammalian Chinese hamster ovary cells. Carcinogenesis. 2017 Mar 1;38(3):336-345. doi: 10.1093/carcin/bgx009

Chen X, Wang J, Qin Q, Jiang Y, Yang G, Rao K, Wang Q, Xiong W, Yuan J. Mono-2-ethylhexyl phthalate induced loss of mitochondrial membrane potential and activation of Caspase 3 in HepG2 cells. Environ Toxicol Pharmacol. 2012 May;33(3):421-30. doi: 10.1016/j.etap.2012.02.001

Chen H, Zhang W, Rui BB, Yang SM, Xu WP, Wei W. Di(2-ethylhexyl) phthalate exacerbates non-alcoholic fatty liver in rats and its potential mechanisms. Environ Toxicol Pharmacol. 2016 Mar;42:38-44. doi: 10.1016/j.etap.2015.12.016

Choi K, Joo H, Campbell JL Jr, Clewell RA, Andersen ME, Clewell HJ 3rd. In vitro metabolism of di(2-ethylhexyl) phthalate (DEHP) by various tissues and cytochrome P450s of human and rat. Toxicol In Vitro. 2012 Mar;26(2):315-22. doi: 10.1016/j.tiv.2011.12.002

Collin A, Hardonnière K, Chevanne M, Vuillemin J, Podechard N, Burel A, Dimanche-Boitrel MT, Lagadic-Gossmann D, Sergent O. Cooperative interaction of benzo[a]pyrene and ethanol on plasma membrane remodeling is responsible for enhanced oxidative stress and cell death in primary rat hepatocytes. Free Radic Biol Med. 2014 Jul;72:11-22. doi: 10.1016/j.freeradbiomed.2014.03.029

Cornell NW, Hansch C, Kim KH, Henegar K. The inhibition of alcohol dehydrogenase in vitro and in isolated hepatocytes by 4-substituted pyrazoles, Arch. Biochem. Biophys. 1983; 227:81-90.

Crabb DW, Bosron WF, Li TK. Ethanol metabolism, Pharmacol. Ther. 1987; 34:59-73.

Decaens C, Rodriguez P, Bouchaud C, Cassio D. Establishment of hepatic cell polarity in the rat hepatoma-human fibroblast hybrid WIF-B9. A biphasic phenomenon going from a simple epithelial polarized phenotype to an hepatic polarized one. J Cell Sci. 1996 Jun;109 (Pt 6):1623-35.

Dirven HA, van den Broek PH, Peters JG, Noordhoek J, Jongeneelen FJ. Microsomal lauric acid hydroxylase activities after treatment of rats with three classical cytochrome P450 inducers and peroxisome proliferating compounds. Biochem Pharmacol. 1992 Jun 23;43(12):2621-9.

Dranka BP, Benavides GA, Diers AR, Giordano S, Zelickson BR, Reily C, Zou L, Chatham JC, Hill BG, Zhang J, Landar A, Darley-Usmar VM. Assessing bioenergetic function in response to oxidative stress by metabolic profiling. Free Radic Biol Med. 2011 Nov 1;51(9):1621-35. doi: 10.1016/j.freeradbiomed.2011.08.005

Ekstedt M, Franzén LE, Mathiesen UL, Thorelius L, Holmqvist M, Bodemar G, Kechagias S. Long-term follow-up of patients with NAFLD and elevated liver enzymes. Hepatology. 2006 Oct;44(4):865-73. doi: 10.1002/hep.21327

Engin A. Non-Alcoholic Fatty Liver Disease, Adv. Exp. Med. Biol. 2017; 960: 443-467. doi: 10.1007/978-3-319-48382-5_19

Estes C, Razavi H, Loomba R, Younossi Z, Sanyal AJ. Modeling the epidemic of nonalcoholic fatty liver disease demonstrates an exponential increase in burden of disease. Hepatology. 2018 Jan;67(1):123-133. doi: 10.1002/hep.29466

Farmer DS, Burcham P, Marin PD. The ability of thiourea to scavenge hydrogen peroxide and hydroxyl radicals during the intra-coronal bleaching of bloodstained root-filled teeth. Aust. Dent. J. 2006; 51:146-152.

Fazakerley DJ, Minard AY, Krycer JR, Thomas KC, Stöckli J, Harney DJ, Burchfield JG, Maghzal GJ, Caldwell ST, Hartley RC, Stocker R, Murphy MP, James DE. Mitochondrial oxidative stress causes insulin resistance without disrupting oxidative phosphorylation. J Biol Chem. 2018 May 11;293(19):7315-7328. doi: 10.1074/jbc.RA117.001254

Foulds CE, Treviño LS, York B, Walker CL. Endocrine-disrupting chemicals and fatty liver disease. Nat Rev Endocrinol. 2017 Aug;13(8):445-457. doi: 10.1038/nrendo.2017.42

Frederiksen H, Skakkebaek NE, Andersson AM. Metabolism of phthalates in humans. Mol Nutr Food Res. 2007 Jul;51(7):899-911. doi : 10.1002/mnfr.200600243

Gao D, Wei C, Chen L, Huang J, Yang S, Diehl AM. Oxidative DNA damage and DNA repair enzyme expression are inversely related in murine models of fatty liver disease. Am J Physiol Gastrointest Liver Physiol. 2004 Nov;287(5):G1070-7. doi: 10.1152/ajpgi.00228.2004

García-Ruiz C, Fernández-Checa JC. Mitochondrial Oxidative Stress and Antioxidants Balance in Fatty Liver Disease. Hepatol Commun. 2018 Oct 30;2(12):1425-1439. doi: 10.1002/hep4.1271

García-Ruiz I, Solís-Muñoz P, Fernández-Moreira D, Grau M, Muñoz-Yagüe T, Solís-Herruzo JA. NADPH oxidase is implicated in the pathogenesis of oxidative phosphorylation dysfunction in mice fed a high-fat diet. Sci Rep. 2016 May 13;6:23664. doi: 10.1038/srep23664

Gitlin JD. Transcriptional regulation of ceruloplasmin gene expression during inflammation. J Biol Chem. 1988 May 5;263(13):6281-7.

Grün F. Obesogens. Curr Opin Endocrinol Diabetes Obes. 2010 Oct;17(5):453-9. doi: 10.1097/MED.0b013e32833ddea0

Ha M, Wei L, Guan X, Li L, Liu C. p53-dependent apoptosis contributes to di-(2-ethylhexyl) phthalate-induced hepatotoxicity. Environ Pollut. 2016 Jan;208(Pt B):416-25. doi: 10.1016/j.envpol.2015.10.009

Hardwick JP. Cytochrome P450 omega hydroxylase (CYP4) function in fatty acid metabolism and metabolic diseases. Biochem Pharmacol. 2008 Jun 15;75(12):2263-75. doi: 10.1016/j.bcp.2008.03.004

Hardwick JP, Osei-Hyiaman D, Wiland H, Abdelmegeed MA, Song BJ. PPAR/RXR Regulation of Fatty Acid Metabolism and Fatty Acid omega-Hydroxylase (CYP4) Isozymes: Implications for Prevention of Lipotoxicity in Fatty Liver Disease. PPAR Res. 2009;2009:952734. doi: 10.1155/2009/952734

Heindel JJ, Blumberg B, Cave M, Machtinger R, Mantovani A, Mendez MA, Nadal A, Palanza P, Panzica G, Sargis R, Vandenberg LN, Vom Saal F. Metabolism disrupting chemicals and metabolic disorders. Reprod Toxicol. 2017 Mar;68:3-33. doi: 10.1016/j.reprotox.2016.10.001

Huff M, da Silveira WA, Carnevali O, Renaud L, Hardiman G. Systems Analysis of the Liver Transcriptome in Adult Male Zebrafish Exposed to the Plasticizer (2-Ethylhexyl) Phthalate (DEHP). Sci Rep. 2018 Feb 1;8(1):2118. doi: 10.1038/s41598-018-20266-8

Imran M, Sergent O, Tête A, Gallais I, Chevanne M, Lagadic-Gossmann D, Podechard N. Membrane Remodeling as a Key Player of the Hepatotoxicity Induced by Co-Exposure to Benzo[a]pyrene and Ethanol of Obese Zebrafish Larvae. Biomolecules. 2018 May 14;8(2). pii: E26. doi: 10.3390/biom8020026

Ip E, Farrell GC, Robertson G, Hall P, Kirsch R, Leclercq I. Central role of PPARalpha-dependent hepatic lipid turnover in dietary steatohepatitis in mice. Hepatology. 2003 Jul;38(1):123-32.

Ito O, Nakamura Y, Tan L, Ishizuka T, Sasaki Y, Minami N, Kanazawa M, Ito S, Sasano H, Kohzuki M. Expression of cytochrome P-450 4 enzymes in the kidney and liver: regulation by PPAR and species-difference between rat and human. Mol Cell Biochem. 2006 Mar;284(1-2):141-8. Epub 2006 Mar 22. Erratum in: Mol Cell Biochem. 2007 May;299(1-2):1-3.

Kamstra JH, Sales LB, Aleström P, Legler J. Differential DNA methylation at conserved non-genic elements and evidence for transgenerational inheritance following developmental exposure to mono(2-ethylhexyl) phthalate and 5-azacytidine in zebrafish. Epigenetics Chromatin. 2017 Apr 12;10:20. doi: 10.1186/s13072-017-0126-4

Kelner MJ, Bagnell R, Welch KJ. Thioureas react with superoxide radicals to yield a sulfhydryl compound. Explanation for protective effect against paraquat. J. Biol. Chem. 1990; 265:1306-1311.

Keys DA, Wallace DG, Kepler TB, Conolly RB. Quantitative evaluation of alternative mechanisms of blood and testes disposition of di(2-ethylhexyl) phthalate and mono(2-ethylhexyl) phthalate in rats. Toxicol Sci. 1999 Jun;49(2):172-85. doi: 10.1093/toxsci/49.2.172

Kurose I, Higuchi H, Kato S, Miura S, Ishii H. Ethanol-induced oxidative stress in the liver, Alcohol Clin. Exp. Res. 1996; 20(1 Suppl):77A-85A.

Lake BG, Gangolli SD, Grasso P, Lloyd AG. Studies on the hepatic effects of orally administered di-)2-ethylhexyl) phthalate in the rat. Toxicol Appl Pharmacol. 1975 May;32(2):355-67.

Latini G, De Felice C, Presta G, Del Vecchio A, Paris I, Ruggieri F, Mazzeo P. Exposure to Di(2-ethylhexyl)phthalate in humans during pregnancy. A preliminary report. Biol Neonate. 2003;83(1):22-4.

Leclercq IA, Farrell GC, Field J, Bell DR, Gonzalez FJ, Robertson GR. CYP2E1 and CYP4A as microsomal catalysts of lipid peroxides in murine nonalcoholic steatohepatitis. J Clin Invest. 2000 Apr;105(8):1067-75.

Le Magueresse-Battistoni B, Labaronne E, Vidal H, Naville D. Endocrine disrupting chemicals in mixture and obesity, diabetes and related metabolic disorders. World J Biol Chem. 2017 May 26;8(2):108-119. doi: 10.4331/wjbc.v8.i2.108

Li Y, Zhang Q, Fang J, Ma N, Geng X, Xu M, Yang H, Jia X. Hepatotoxicity study of combined exposure of DEHP and ethanol: A comprehensive analysis of transcriptomics and metabolomics. Food Chem Toxicol. 2020 Apr 20:111370. doi: 10.1016/j.fct.2020.111370. [Epub ahead of print]

Liamin M, Boutet-Robinet E, Jamin EL, Fernier M, Khoury L, Kopp B, Le Ferrec E, Vignard J, Audebert M, Sparfel L. Benzo[a]pyrene-induced DNA damage associated with mutagenesis in primary human activated T lymphocytes. Biochem Pharmacol. 2017 Aug 1;137:113-124. doi: 10.1016/j.bcp.2017.04.025

Lieber CS. The discovery of the microsomal ethanol oxidizing system and its physiologic and pathologic role. Drug Metab Rev. 2004 Oct;36(3-4):511-29.

Liu N, Jiang L, Sun X, Yao X, Zhai X, Liu X, Wu X, Bai Y, Wang S, Yang G. Mono-(2-ethylhexyl) phthalate induced ROS-dependent autophagic cell death in human vascular endothelial cells. Toxicol In Vitro. 2017 Oct;44:49-56. doi: 10.1016/j.tiv.2017.06.024

Lu Y, Cederbaum AI. CYP2E1 and oxidative liver injury by alcohol. Free Radic Biol Med. 2008 Mar 1;44(5):723-38.

Melnick RL, Schiller CM. Mitochondrial toxicity of phthalate esters. Environ Health Perspect. 1982 Nov;45:51-6.

Milošević N, Milanović M, Sudji J, Bosić Živanović D, Stojanoski S, Vuković B, Milić N, Medić Stojanoska M. Could phthalates exposure contribute to the development of metabolic syndrome and liver disease in humans? Environ Sci Pollut Res Int. 2020 Jan;27(1):772-784. doi: 10.1007/s11356-019-06831-2

Nazir DJ, Alcaraz AP, Bierl BA, Beroza M, Nair PP. Isolation, identification, and specific localization of di-2-ethylhexyl phthalate in bovine heart muscle mitochondria. Biochemistry. 1971 Nov;10(23):4228-32.

Park EC, Kim SI, Hong Y, Hwang JW, Cho GS, Cha HN, Han JK, Yun CH, Park SY, Jang IS, Lee ZW, Choi JS, Kim S, Kim GH. Inhibition of CYP4A reduces hepatic endoplasmic reticulum stress and features of diabetes in mice. Gastroenterology. 2014 Oct;147(4):860-9. doi: 10.1053/j.gastro.2014.06.039

Park CG, Sung B, Ryu CS, Kim YJ. Mono-(2-ethylhexyl) phthalate induces oxidative stress and lipid accumulation in zebrafish liver cells. Comp Biochem Physiol C Toxicol Pharmacol. 2020 Apr;230:108704. doi: 10.1016/j.cbpc.2020.108704

Patel V, Sanyal AJ, Sterling R. Clinical Presentation and Patient Evaluation in Nonalcoholic Fatty Liver Disease. Clin Liver Dis. 2016 May;20(2):277-92. doi: 10.1016/j.cld.2015.10.006

Pessayre D, Fromenty B. NASH: a mitochondrial disease. J Hepatol. 2005 Jun;42(6):928-40.

Podechard N, Chevanne M, Fernier M, Tête A, Collin A, Cassio D, Kah O, Lagadic-Gossmann D, Sergent O. Zebrafish larva as a reliable model for in vivo assessment of membrane remodeling involvement in the hepatotoxicity of chemical agents. J Appl Toxicol. 2017 Jun;37(6):732-746. doi: 10.1002/jat.3421

Pospisilik JA, Knauf C, Joza N, Benit P, Orthofer M, Cani PD, Ebersberger I, Nakashima T, Sarao R, Neely G, Esterbauer H, Kozlov A, Kahn CR, Kroemer G, Rustin P, Burcelin R, Penninger JM. Targeted deletion of AIF decreases mitochondrial oxidative phosphorylation and protects from obesity and diabetes. Cell. 2007 Nov 2;131(3):476-91.

Reinehr R, Becker S, Eberle A, Grether-Beck S, Häussinger D. Involvement of NADPH oxidase isoforms and Src family kinases in CD95-dependent hepatocyte apoptosis. J Biol Chem. 2005 Jul 22;280(29):27179-94.

Rusyn I, Corton JC. Mechanistic considerations for human relevance of cancer hazard of di(2-ethylhexyl) phthalate. Mutat Res. 2012 Apr-Jun;750(2):141-58. doi: 10.1016/j.mrrev.2011.12.004

Ryu JS, Lee M, Mun SJ, Hong SH, Lee HJ, Ahn HS, Chung KS, Kim GH, Son MJ. Targeting CYP4A attenuates hepatic steatosis in a novel multicellular organotypic liver model. J Biol Eng. 2019 Aug 8;13:69. doi: 10.1186/s13036-019-0198-8

Sahini N, Borlak J. Recent insights into the molecular pathophysiology of lipid droplet formation in hepatocytes. Prog Lipid Res. 2014 Apr;54:86-112. doi: 10.1016/j.plipres.2014.02.002

Sanyal AJ, Brunt EM, Kleiner DE, Kowdley KV, Chalasani N, Lavine JE, Ratziu V, McCullough A. Endpoints and clinical trial design for nonalcoholic steatohepatitis. Hepatology. 2011 Jul;54(1):344-53. doi: 10.1002/hep.24376

Seki T, Wang MH, Miyata N, Laniado-Schwartzman M. Cytochrome P450 4A isoform inhibitory profile of N-hydroxy-N'-(4-butyl-2-methylphenyl)-formamidine (HET0016), a selective inhibitor of 20-HETE synthesis. Biol Pharm Bull. 2005 Sep;28(9):1651-4.

Sergent O, Pereira M, Belhomme C, Chevanne M, Huc L, Lagadic-Gossmann D. Role for membrane fluidity in ethanol-induced oxidative stress of primary rat hepatocytes. J. Pharmacol. Exp. Ther. 2005; 313:104-111. doi: 10.1124/jpet.104.078634

Siegel AB, Zhu AX. Metabolic syndrome and hepatocellular carcinoma: Two growing epidemics with a potential link. Cancer. 2009 Dec 15;115(24):5651-61. doi: 10.1002/cncr.24687

Simpson AE. The cytochrome P450 4 (CYP4) family. Gen Pharmacol. 1997 Mar;28(3):351-9.

Spahis S, Delvin E, Borys JM, Levy E. Oxidative Stress as a Critical Factor in Nonalcoholic Fatty Liver Disease Pathogenesis, Antioxid. Redox Signal. 2017; 26:519-541. doi: 10.1089/ars.2016.6776

Swaminathan K, Clemens DL, Dey A. Inhibition of CYP2E1 leads to decreased malondialdehyde-acetaldehyde adduct formation in VL-17A cells under chronic alcohol exposure, Life Sci. 2013; 92: 325-336. doi: 10.1016/j.lfs.2012.12.014

Tête A, Gallais I, Imran M, Chevanne M, Liamin M, Sparfel L, Bucher S, Burel A, Podechard N, Appenzeller BMR, Fromenty B, Grova N, Sergent O, Lagadic-Gossmann D. Mechanisms involved in the death of steatotic WIF-B9 hepatocytes co-exposed to benzo[a]pyrene and ethanol: a possible key role for xenobiotic metabolism and nitric oxide. Free Radic Biol Med. 2018 Dec;129:323-337. doi: 10.1016/j.freeradbiomed.2018.09.042

Thomas JA, Northup SJ. Toxicity and metabolism of monoethylhexyl phthalate and diethylhexyl phthalate: a survey of recent literature. J Toxicol Environ Health. 1982 Jan;9(1):141-52.

Thurman RG, McKenna WR. Pathways of ethanol metabolism in perfused rat liver. Adv Exp Med Biol. 1975;56:57-76.

Tsai CF, Hsieh TH, Lee JN, Hsu CY, Wang YC, Lai FJ, Kuo KK, Wu HL, Tsai EM, Kuo PL. Benzyl butyl phthalate induces migration, invasion, and angiogenesis of Huh7 hepatocellular carcinoma cells through nongenomic AhR/G-protein signaling. BMC Cancer. 2014 Aug 1;14:556. doi: 10.1186/1471-2407-14-556

Vornoli A, Pozzo L, Della Croce CM, Gervasi PG, Longo V. Drug metabolism enzymes in a steatotic model of rat treated with a high fat diet and a low dose of streptozotocin. Food Chem Toxicol. 2014 Aug;70:54-60. doi: 10.1016/j.fct.2014.04.042

Wahlang B, Beier JI, Clair HB, Bellis-Jones HJ, Falkner KC, McClain CJ, Cave MC. Toxicant-associated steatohepatitis. Toxicol Pathol. 2013 Feb;41(2):343-60. doi: 10.1177/0192623312468517

Wahlang B, Jin J, Beier JI, Hardesty JE, Daly EF, Schnegelberger RD, Falkner KC, Prough RA, Kirpich IA, Cave MC. Mechanisms of Environmental Contributions to Fatty Liver Disease. Curr Environ Health Rep. 2019 Sep;6(3):80-94. doi: 10.1007/s40572-019-00232-w

Wang Y, Zhu H, Kannan K. A Review of Biomonitoring of Phthalate Exposures. Toxics. 2019 Apr 5;7(2). pii: E21. doi: 10.3390/toxics7020021

Wójtowicz AK, Szychowski KA, Wnuk A, Kajta M. Dibutyl Phthalate (DBP)-Induced Apoptosis and Neurotoxicity are Mediated via the Aryl Hydrocarbon Receptor (AhR) but not by Estrogen Receptor Alpha (ERα), Estrogen Receptor Beta (ERβ), or Peroxisome Proliferator-Activated Receptor Gamma (PPARγ) in Mouse Cortical Neurons. Neurotox Res. 2017 Jan;31(1):77-89. doi: 10.1007/s12640-016-9665-x

Wormuth M, Scheringer M, Vollenweider M, Hungerbühler K. What are the sources of exposure to eight frequently used phthalic acid esters in Europeans? Risk Anal. 2006 Jun;26(3):803-24. doi: 10.1111/j.1539-6924.2006.00770.x

Xu Y, Agrawal S, Cook TJ, Knipp GT. Maternal di-(2-ethylhexyl)-phthalate exposure influences essential fatty acid homeostasis in rat placenta. Placenta. 2008 Nov;29(11):962-9. doi: 10.1016/j.placenta.2008.08.011

Yang G, Zhang W, Qin Q, Wang J, Zheng H, Xiong W, Yuan J. Mono(2-ethylhexyl) phthalate induces apoptosis in p53-silenced L02 cells via activation of both mitochondrial and death receptor pathways. Environ Toxicol. 2015 Sep;30(10):1178-91. doi: 10.1002/tox.21990

Yang G, Zhou X, Wang J, Zhang W, Zheng H, Lu W, Yuan J. MEHP-induced oxidative DNA damage and apoptosis in HepG2 cells correlates with p53-mediated mitochondria-dependent signaling pathway. Food Chem Toxicol. 2012 Jul;50(7):2424-31. doi: 10.1016/j.fct.2012.04.023

Yokoyama Y, Okubo T, Kano I, Sato S, Kano K. Induction of apoptosis by mono(2-ethylhexyl)phthalate (MEHP) in U937 cells. Toxicol Lett. 2003 Oct 15;144(3):371-81.

Younossi Z, Henry L. Contribution of alcoholic and nonalcoholic fatty liver disease to the burden of liver-related morbidity and mortality. Gastroenterology. 2016a Jun;150(8):1778-85. doi: 10.1053/j.gastro.2016.03.005

Younossi ZM, Koenig AB, Abdelatif D, Fazel Y, Henry L, Wymer M. Global epidemiology of nonalcoholic fatty liver disease-Meta-analytic assessment of prevalence, incidence, and outcomes. Hepatology. 2016b Jul;64(1):73-84. doi: 10.1002/hep.28431

Younossi ZM, Otgonsuren M, Henry L, Venkatesan C, Mishra A, Erario M, Hunt S. Association of nonalcoholic fatty liver disease (NAFLD) with hepatocellular carcinoma (HCC) in the United States from 2004 to 2009. Hepatology. 2015 Dec;62(6):1723-30. doi: 10.1002/hep.28123

Zhang X, Li S, Zhou Y, Su W, Ruan X, Wang B, Zheng F, Warner M, Gustafsson JÅ, Guan Y. Ablation of cytochrome P450 omega-hydroxylase 4A14 gene attenuates hepatic steatosis and fibrosis. Proc Natl Acad Sci U S A. 2017a Mar 21;114(12):3181-3185. doi: 10.1073/pnas.1700172114

Zhang W, Shen XY, Zhang WW, Chen H, Xu WP, Wei W. The effects of di 2-ethyl hexyl phthalate (DEHP) on cellular lipid accumulation in HepG2 cells and its potential mechanisms in the molecular level. Toxicol Mech Methods. 2017b May; 27(4):245-252. doi: 10.1080/15376516.2016.1273427

Zhang Y, Wang S, Zhao T, Yang L, Guo S, Shi Y, Zhang X, Zhou L, Ye L. Mono-2-ethylhexyl phthalate (MEHP) promoted lipid accumulation via JAK2/STAT5 and aggravated oxidative stress in BRL-3A cells. Ecotoxicol Environ Saf. 2019 Nov 30;184:109611. doi: 10.1016/j.ecoenv.2019.109611

FIGURE LEGENDS

Figure 1. Role for caspases 3/7 in the cell death of steatotic WIF-B9 cells co-exposed to MEHP and ethanol. Prior steatosis was induced **(A-D)** or not **(A,B)** by a 2-days incubation with palmitic acid (450 µM) and oleic acid (100 µM). Non-steatotic or steatotic hepatocytes were treated or not (C; control cells treated with DMSO) with 5 mM ethanol (E), 500 nM MEHP (M) or a combination of both toxicants (ME) for 5 days. Apoptosis was evaluated by counting cells with condensed/fragmented chromatin after nuclear staining with Hoechst 33342 in presence **(C)** or not **(A, C)** of a pan-caspase inhibitor zVAD (10 µM), and by analyzing DEVDase activities of caspases 3/7 by spectrofluorimetry **(D)**. Necrosis was evaluated by counting cells positive for Sytox Green staining, a green-fluorescent dye **(B).** In **(E)**, caspase-3 cleavage was detected by western-blotting upon MEHP alone and co-exposure. All results are means ± SD for at least three independent cultures (except for (E), n=1). #: Significantly different from condition without prior steatosis. a: Significantly different from corresponding control (with or without steatosis). b: Significantly different from MEHP alone. *: Significantly different from condition without inhibitor (zVAD).

Figure 2. Role for DNA damage-related p53 activation in the cell death of steatotic WIF-B9 cells co-exposed to MEHP and ethanol. Steatotic hepatocytes were treated or not (C; treated with DMSO) with 5 mM ethanol (E), 500 nM MEHP (M) or a combination of both toxicants (ME) for 5 days. DNA damage was evaluated by analyzing the phosphorylation of H2AX on Ser139 (γH2AX) by immunocytochemistry **(A).** Evaluation of p53 involvement in cell death was realized by testing the effect of the p53 inhibitor pifithrin α (PFT; 10 µM) on apoptosis **(B)**. Apoptosis was evaluated by counting cells with condensed/fragmented chromatin after nuclear staining with Hoechst 33342. Fluorescence microscopy analysis and quantification of cell number with nuclear p53 protein localization **(C and D)**. Confirmation of p53 activation by western blotting of Ser15-phospho-p53 (P-p53) from total cell lysates **(E)**. All results are means ± SD for at least three independent cultures (except for (E), n=1). a: Significantly different from corresponding control. b: Significantly different from MEHP alone. *: Significantly different from condition without inhibitor (PFT).

Figure 3. Involvement of ethanol metabolism in the cell death induced by MEHP/ethanol co-exposure in steatotic WIF-B9 cells. Non-steatotic or steatotic hepatocytes were treated or not (C; treated with DMSO) with 5 mM ethanol (E), 500 nM MEHP (M) or a combination of both toxicants (ME) for 5 days **(A,B)** or 3 h **(C,D)**, in presence or not of inhibitor. The involvement of ethanol metabolism was analyzed by testing the effect of the CYP2E1/ADH inhibitor 4-methylpyrazole (4-MP, 500 µM), on **(A)** apoptosis after Hoechst 33342 staining. **(B)** CYP2E1 activity was assessed by HPLC analyses (UV detection) of the formation of chlorzoxazone O-glucuronide (OCZX) (*cf.* Tête at *al.*, for Methods). ADH activity was evaluated by measuring the NADH production by spectrophotometry **(C).** This activity was given relative to control cells. **(D)** *ADH 1,4,5* and *7* mRNA expression was evaluated by RT-qPCR. Data were given relative to mRNA level in non-steatotic control (C) cells. Results are means ± SD for at least three independent cultures. #: Significantly different from condition without prior steatosis. a: Significantly different from corresponding control (with or without steatosis). b: Significantly different from MEHP alone. *: Significantly different from condition without inhibitor (4-MP).

Figure 4. Role for AhR in the cell damages induced by MEHP/ethanol co-exposure in steatotic WIF-B9 cells. Steatotic hepatocytes were treated or not (C; treated with DMSO) with 5 mM ethanol (E), 500 nM MEHP (M) or a combination of both toxicants (ME) for 3 h **(A)**, or for 5 days **(B,C)** in presence or not of inhibitor. The involvement of AhR activation was analyzed by testing the effect of the specific antagonist CH-223191 (CH; 3 µM) on **(A)** ADH activity evaluated by measuring the NADH production by spectrophotometry (activity given relative to control), **(B)** DNA damage evaluated by analyzing the phosphorylation of H2AX on Ser139 (γH2AX) by immunocytochemistry, and **(C)** apoptosis after Hoechst 33342 staining. In **(C)**, the effect of another AhR antagonist, namely α-Naphthoflavone (αNF, 10 µM) was also tested. Results are means ± SD for at least three independent cultures. a: Significantly different from corresponding control (with or without steatosis). b: Significantly different from MEHP alone. *: Significantly different from condition without inhibitor (CH or αNF).

Figure 5. Involvement of CYP4A in the cell death induced by MEHP/ethanol co-exposure in steatotic WIF-B9 cells. Non-steatotic or steatotic hepatocytes were treated or not (C; treated with DMSO) with 5 mM ethanol (E), 500 nM MEHP (M) or a combination of both toxicants (ME) for 5 days, in presence or not of inhibitor. The mRNA expression of *Cyp4a1* **(A)**, *4a2* **(B)** and *4a3* **(C)** was evaluated by RT-qPCR, and was given relative to mRNA level in control non-steatotic cells. **(D)** CYP4A protein level was evaluated by western-blotting analysis. Representative western blots and relative band density quantification are illustrated. The involvement of CYP4A was tested by analyzing the effects of the CYP4A inhibitor HET0016 (500 nM) on **(E)** apoptosis evaluated following Hoechst 33342 staining, and (**F**) DNA damage evaluated by counting cells positive for γH2AX staining. Results are means ± SD for at least three independent cultures. #: Significantly different from condition without prior steatosis. a: Significantly different from corresponding control (with or without steatosis). b: Significantly different from MEHP alone. *: Significantly different from condition without HET0016.

Figure 6. Involvement of oxidative stress in the cell death induced by MEHP/ethanol co-exposure in steatotic WIF-B9 cells. Steatotic hepatocytes were treated or not (C; treated with DMSO) with 5 mM ethanol (E), 500 nM MEHP (M) or a combination of both toxicants (ME) for 5 days, in presence or not of antioxidant. The involvement of oxidative stress in toxicity was evaluated by testing the effects of the antioxidant molecule thiourea (6.25 mM) on **(A)** apoptosis after Hoechst 33342 staining, and **(B)** DNA damage evaluated by counting cells positive for γH2AX staining. Lipid peroxidation was assessed by measuring the production of malondialdehyde (MDA) by HPLC **(C)**. The superoxide anion production was assessed by the measurement in fluorescence of 2-OH-ethidium using DHE probe **(D)**. Results are means ± SD for at least three independent cultures. a: Significantly different from control. b: Significantly different from MEHP alone. *: Significantly different from condition without thiourea. F.A.U.: Fluorescence Arbitrary Unit.

Figure 7. Exacerbation of liver damage severity by DEHP/ethanol co-exposure in zebrafish larvae with steatosis. Zebrafish larvae were fed with a standard diet (SD) or a high-fat diet (HFD) from 4 dpf until 12 dpf. From 5 dpf, SD and HFD zebrafish were either left untreated (C), or treated

with 2.56 nM DEHP (D), 43 mM ethanol (E) or a combination of both toxicants (DE) for 7 days. ***(A)*** Liver damages were evaluated on zebrafish liver sections after HES staining (magnification x 400). Damaged/dead cells or ballooned/vacuolated hepatocytes were indicated by red arrows. Images are representative of at least 3 larvae. **(B-E)** mRNA expression of several genes characteristic of liver toxicity (*cf.* Imran *et al*., 2018) after exposing HFD zebrafish larvae to DEHP/ethanol mixture. The mRNA expressions were evaluated by RT-qPCR. Data are expressed relative to mRNA levels found in HFD control larvae, set at 0 (log 2 change). Values are the mean ± SEM of 8 larvae. *Significantly different from untreated, control HFD larvae; [b]Significantly different from HFD larvae treated by DEHP only.

Figure 8. Impact of DEHP/ethanol co-exposure on the expression of several inflammatory markers in zebrafish larvae with steatosis. Larvae were fed with a high-fat diet (HFD) from 4 dpf until 12 dpf. From 5 dpf, HFD zebrafish were either left untreated (C), or treated with 2.56 nM DEHP (D), 43 mM ethanol (E) or a combination of both toxicants (DE) for 7 days. The mRNA expressions were analyzed after exposing HFD zebrafish larvae to DEHP/ethanol mixture or toxicants alone, using RT-qPCR. Data are expressed relative to mRNA levels found in HFD control larvae, set at 0 (log 2 change). Values are the mean ± SEM of 8 larvae. *Significantly different from untreated, control HFD larvae; [b]Significantly different from HFD larvae treated by DEHP only.

Figure 9. Schematic diagram summarizing the deleterious effects of phthalate/ethanol co-exposure in *in vitro* and *in vivo* models of pre-established liver steatosis. Upon co-exposing steatotic WIF-B9 hepatocytes to MEHP and ethanol, both an AhR-dependent increase in ADH activity as well as CYP4A activation would result in oxidative stress, leading to DNA damage and hence a p53-dependent apoptotic cell death. In HFD-zebrafish larvae, DEHP/ethanol co-exposure would lead to liver injuries, reflected by alterations in hepatocytes as well as increased expression of genes related to hepatotoxicity or inflammation. In this context, a transition towards a NASH-like state might be put forward upon phthalate/ethanol co-exposure of prior liver steatosis. Regarding the mechanisms involved in the *in vivo* model, a possible role for *cyp4t8* (homolog gene of CYP4A) mRNA expression might be proposed since an increase in this expression has been observed.

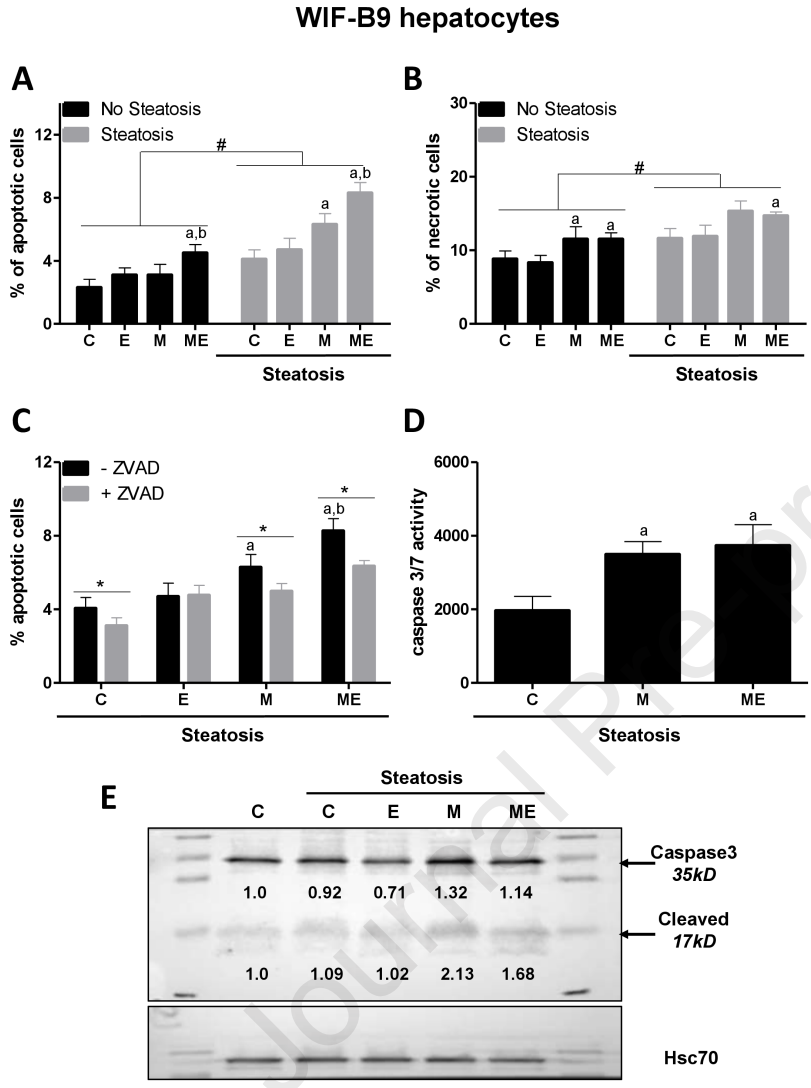

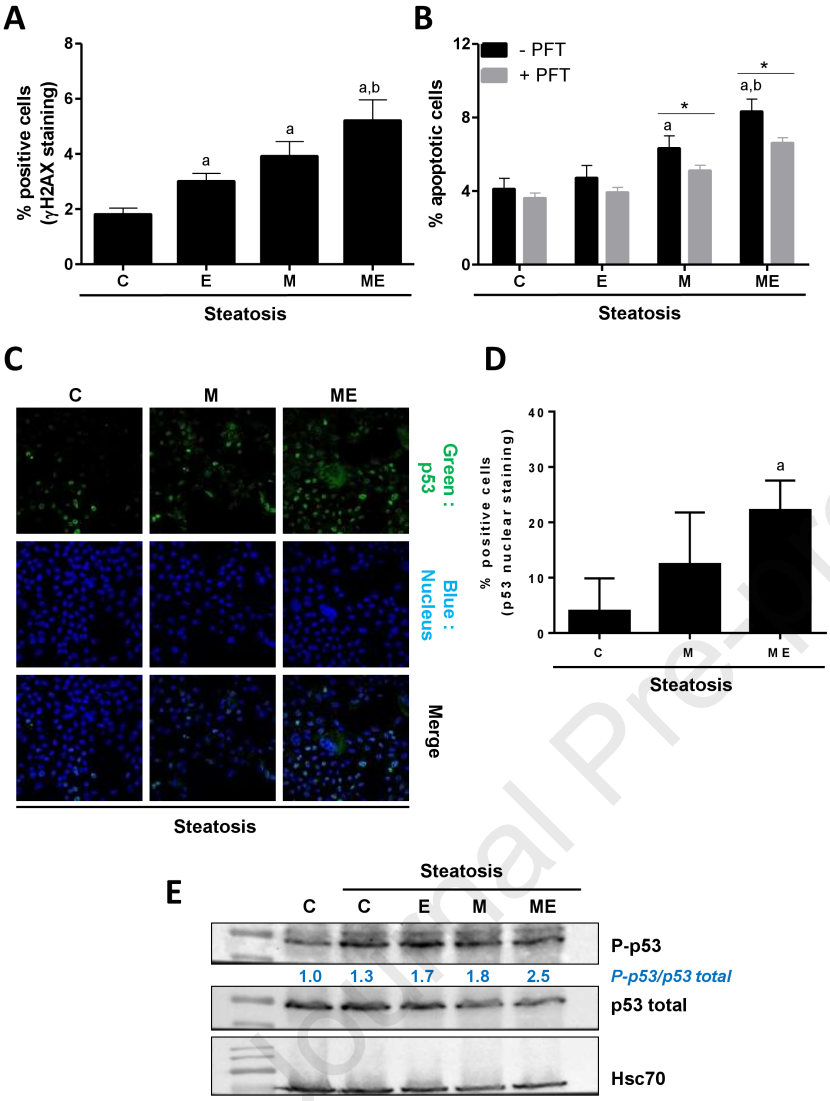

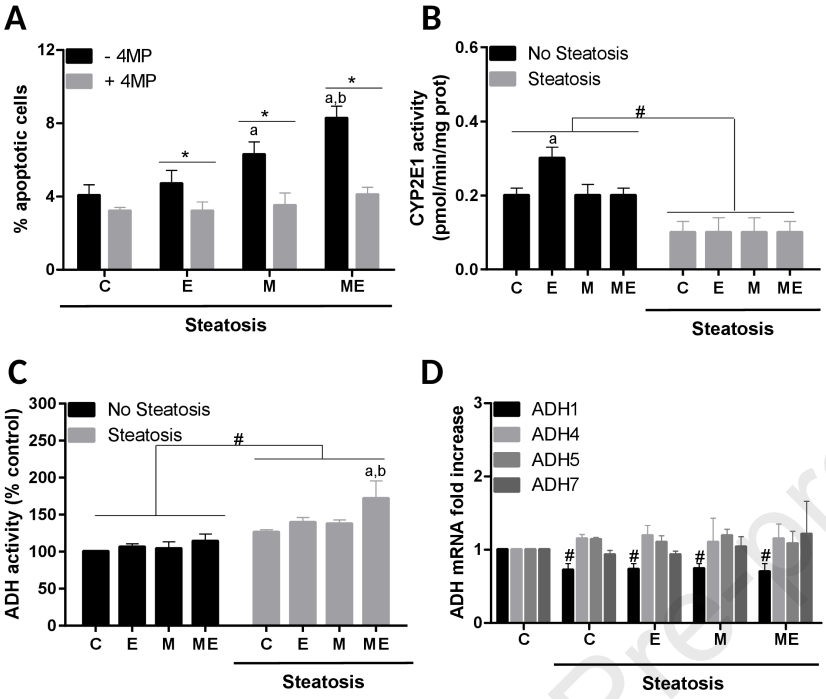

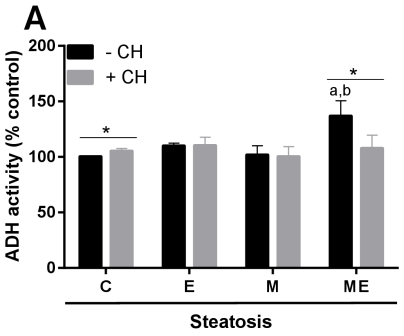

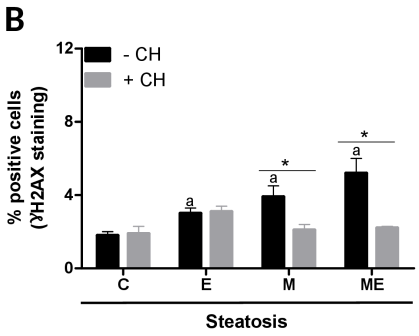

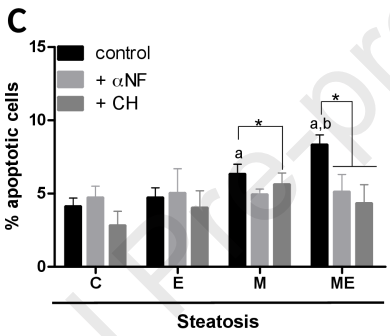

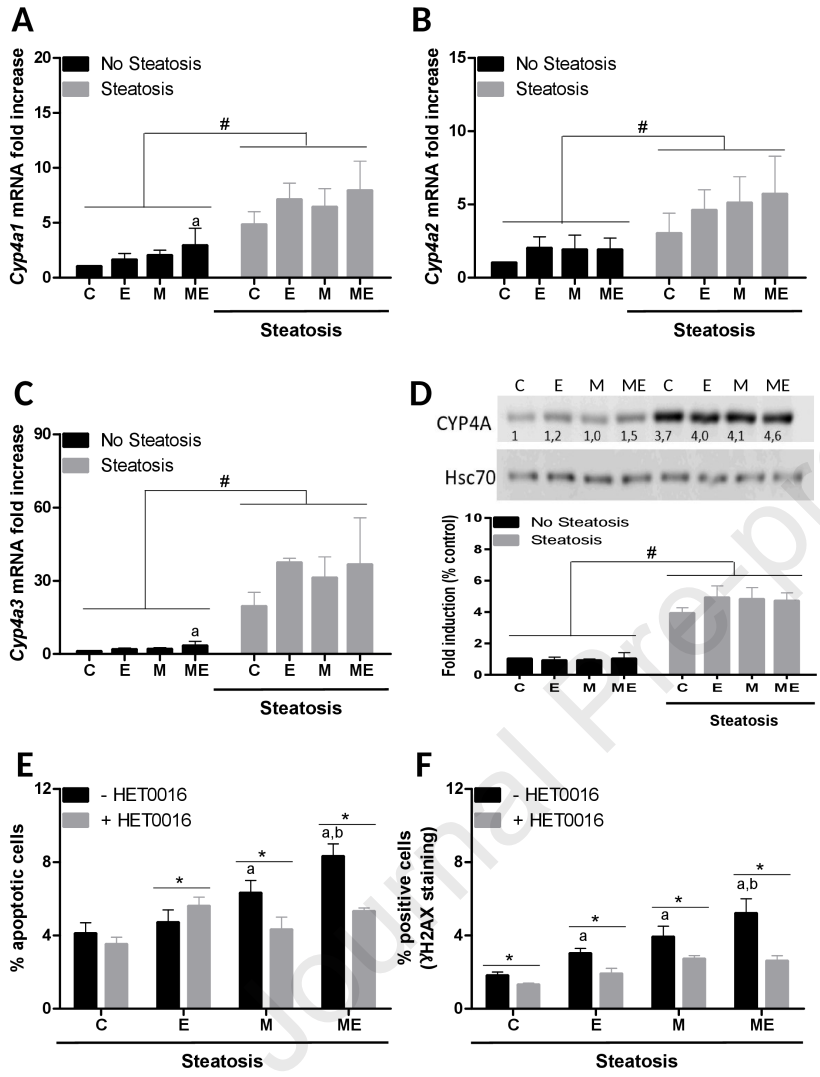

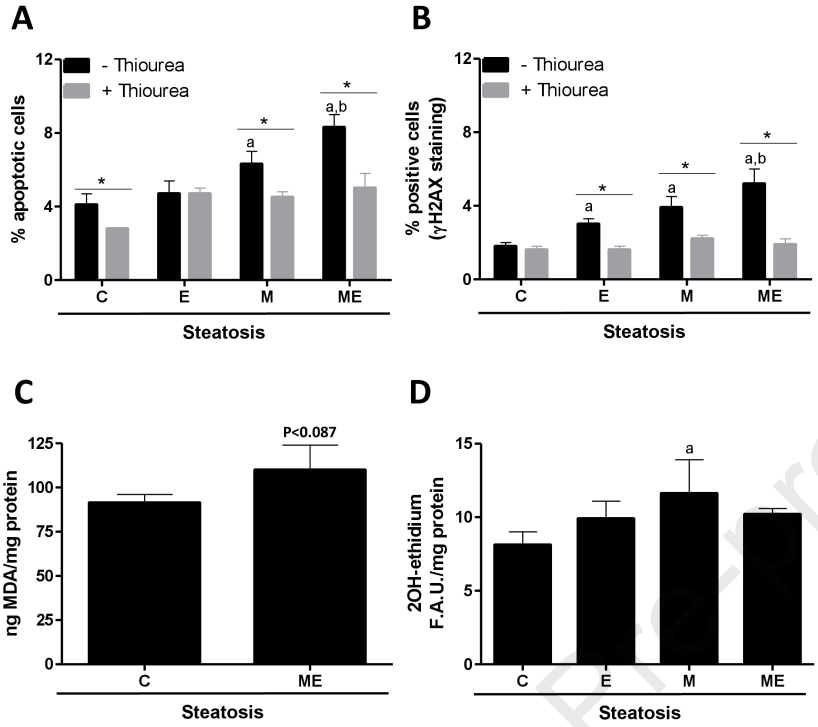

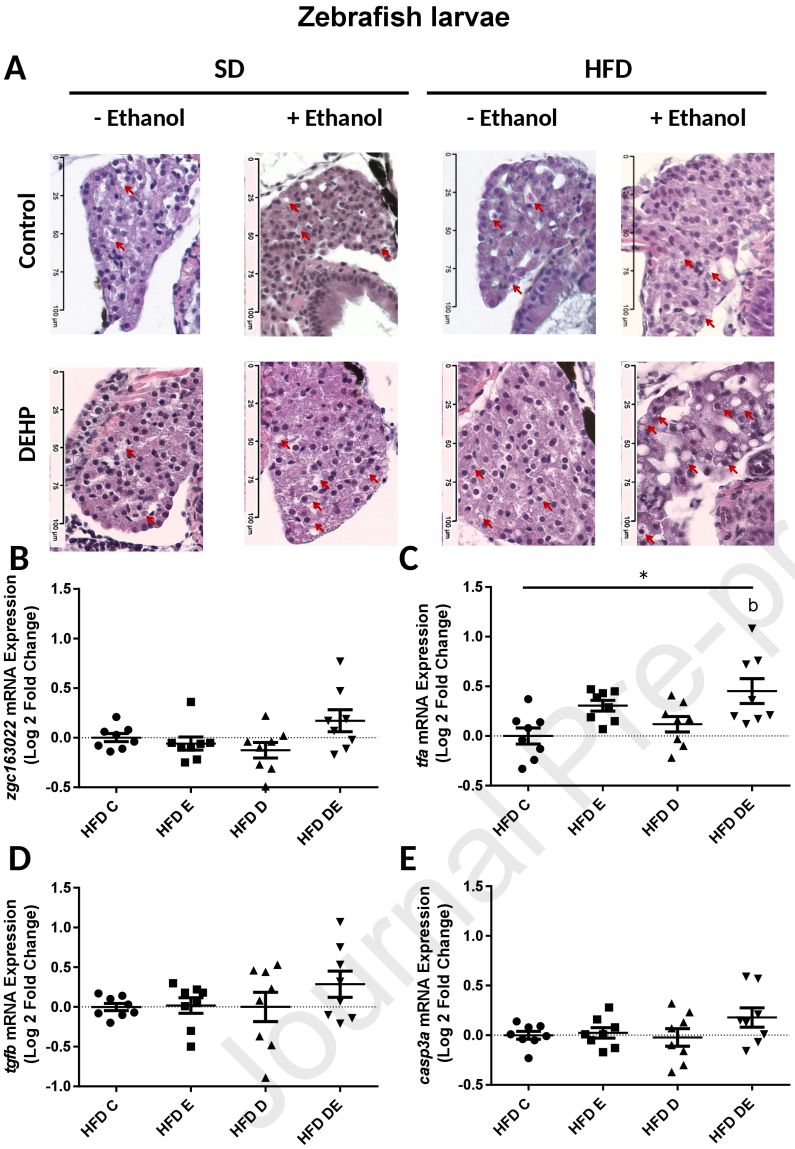

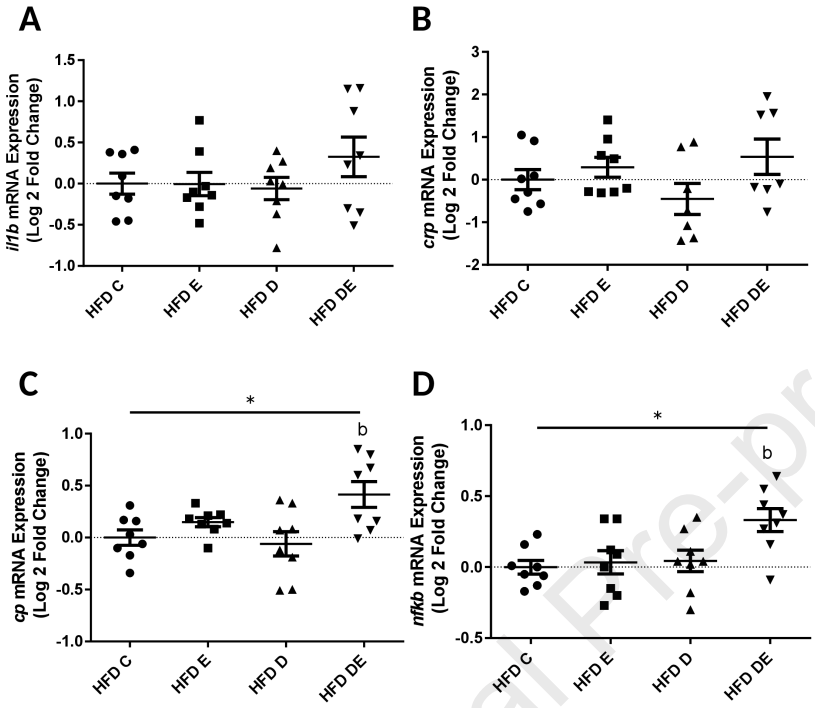

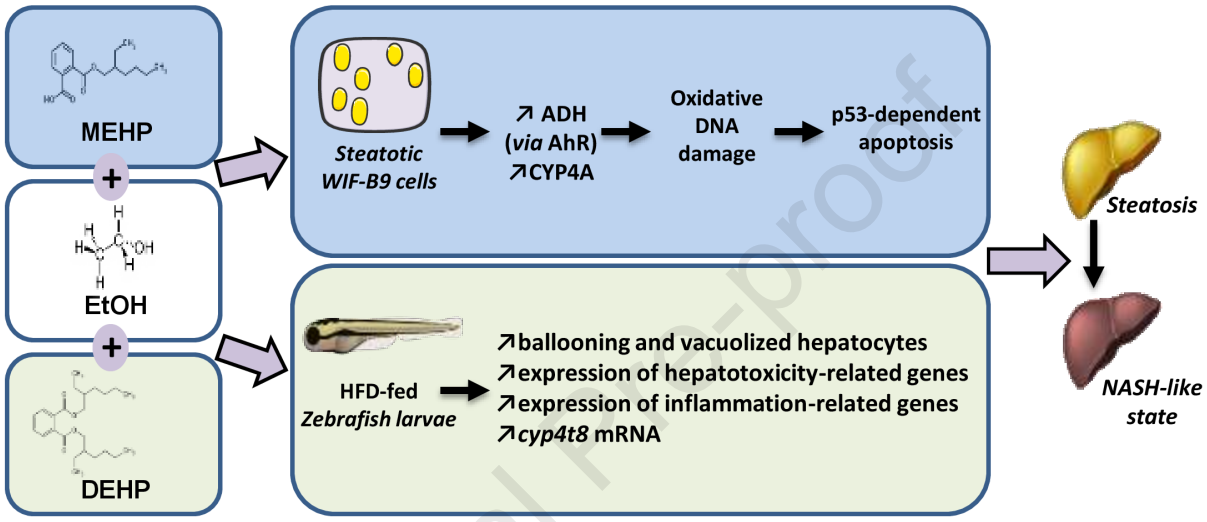

Declaration of interests

☒ The authors declare that they have no known competing financial interests or personal relationships that could have appeared to influence the work reported in this paper.

☐The authors declare the following financial interests/personal relationships which may be considered as potential competing interests: